Université Pierre et Marie Curie, École des Mines de Paris

& École Nationale du Génie Rural des Eaux et des Forêts

Master 2 Sciences de l'Univers, Environnement, Ecologie

Parcours Hydrologie-Hydrogéologie

Snowpack water isotopes in northern Scandinavia during winter 2010 – 2011

Vincent Thiébaut

Steve Lyon and Christophe Sturm

Department of Geology and geochemistry
Stockholm University
106 91 Stockholm, Sweden

Septembre 2011

Abstract

Isotopic composition of precipitation depends on many different parameters. One key parameter, for example, is the origin of the vapor. The wind trajectories bringing air masses over Western Europe are partly influenced by the North Atlantic Oscillation (NAO). As a strong example of this, consider when the NAO index was negative in winter 2009-2010 and winter 2010-2011. In addition to this extremely negative NAO, those two winters were characterized by low temperatures and huge amount of snowfalls.

In this study, fresh snow has been collected in Sweden and Norway roughly between the latitudes 62° N and 68° N after the last snow falls. This covers the period from the 4th of March to the 12th of March 2011. Snow cores have been collected during a field campaign on 20 sites spread over a 350.000km² area representing more than 700 samples. Those snow samples were collected and brought to Stockholm University in order to measure their stable water isotope content ($\delta^{18}O$ and δD). Other parameters like density, snow depth and grain size were also measured or calculated.

The samples were analyzed thanks to a laser spectrometer from Los Gatos Research (LGR-LS). This tool has been commercially available for less than 4 years. This new tool enables quicker and cheaper analysis of isotopic composition of water samples. However, initial evaluation of the LGR-LS after it was delivered to Stockholm University in January 2010 revealed issues about its accuracy. Therefore, a first part of this study aimed to find the best experimental protocol and post-analysis treatment.

The data derived from collected snow is used to investigate the feedbacks between the land surfaces and the atmospheric dynamic. In a previous study, G. Rousseau showed the importance of the westerly air masses effect on the isotopic composition of the snowpack in Scandinavia and its relation to the phenomenon predicted by the $REMO_{ISO}$ model. The winter 2011 data collected in this current study show an even greater isotopic signal.

Furthermore, those data enable us also to have a better understanding of this winter, regarding also the temporal variability of the isotopic signature of the snow pack.

Master 2 Hydrology/hydrogeology at UPMC

STABLE WATER ISOTOPES IN THE NORTHERN SCANDINAVIA SNOWPACK DURING THE WINTER 2010-2011

Snowpack water isotopes, a reflect of the sky ?

Master Thesis

Vincent THIEBAUT

Table of content

List of figures

List of equations

Acknowledgements

My first thanks go to Steve Lyon and Christophe Sturm without whom I would not have been able to carry out his project.

I want to thank also Andrès Peralta Tapia who drove me during this extraordinary trip over the North of Sweden and help me during this whole sampling campaign.

I also would like to thank Heike Siegmund who helped a lot for the technical part of this project and whose advices and knowledge was precious to solve the problems with the laser spectrometer. My thanks go also to Magnus Mörth for the excel makro.

A special thank to my boyfriend Blick for his support and good advices for the redaction of this thesis.

I would like to thank Thibaut, Diego and Francesco and all the other people I met during this seven months.

I am also grateful to the people who hosted us, Andrès and I, during the field trip, Johannes in Trondheim who cooked a nice vegan meal for us. And I must also thank Kamilla, who hosted us in Östersund.

I am also very thankful to Lie who hosted me at the end of this project.

Finally I want to thank my family and friends who encouraged me for this work in Sweden.

A. Introduction

1/ Outline of the study

This report presents the studies done during an internship at the Stockholm University from February 2011 until September 2011. I was supervised by Steve Lyon from the department of Physical Geography and Quaternary Geology and Christophe Sturm from the department of Geological Sciences. This internship consisted of collecting snow cores in the Northern half of Scandinavia and analyzing them at the Stockholm University in order to get the composition of the stable water isotopes (SWI), hydrogen and oxygen.

For the last two years, the North Atlantic Oscillation (NAO) has been extremely negative (Cattiaux et al. 2010). One of the main goals of this study is to link this extreme NAO event to the isotopic composition of the snow pack across Sweden by sampling snow cores. This should provide results giving a better understanding of climatic dynamics and precipitations mechanisms over Sweden during this extremely negative NAO index.

My work also focused on the technical and statistical aspects as we used a relatively new tool to analyze the SWI. This tool is called the Laser spectrometer (LGR-LS). A second goal of this study was therefore to develop a calculation method to minimize bias and errors associated with this machine.

2/ General context

2.I. The Laser-spectrometer

For several decades, Stable water isotopes have been measured thanks to the mass spectrometer which measures the mass-to-charge ratio of charged particles. This tool has a good accuracy but needs much sample preparation, needs much time for the analysis and is fairly expensive. A laser spectrometer, a new tool that has been commercially available for less than 4 years has offers a new technology for the analysis of water stable isotopes. It is twice as fast as the mass spectrometer. Though, initial evaluation revealed issues about the accuracy and errors associated with the machine that need to be estimated. A good experimental protocol has to be developed to improve the accuracy of the laser spectrometer which represents a potential technological breakthrough for stable water isotopes.

2.II. The project

Last year, G. Rousseau was the first to investigate stable water isotope in the snowpack to estimate their ability to allow for comment about the connections between

atmospheric conditions and snowfalls and concluded saying that this methodology has a very big potential.

His project and mine are part of a larger project led by C. STURM drawing upon large amounts of data about hydrology, meteorology and sedimentology. Stable Isotopes are widely used in different fields of study like climatology. Oxygen-18 and Deuterium are the isotopes used in this current work but carbon as well as nitrogen have also been targeted. Even if the stable isotopes have been used for several decades, interpretation of the evolution of isotopes contents in paleo-archive is still debated. Indeed, lots of conclusions about stable isotopes in ice cores or sediment cores are based on the hypothesis that the only parameter governing the isotopes quotas is temperature (Daansgard, 1964). Now we know that climate dynamic and air masses origin are parameters that we cannot neglect when trying to interpret stable isotopes.

C. Sturm and colleagues at Stockholm University aim at investigating the feedbacks between the atmosphere and the land surface by studying the water cycle and transport and transformation of the organic matter thanks to the isotopes ($H_2{}^{18}O$, HDO and also ^{13}C for the O.M.) with an over arching goal to improve the interpretation of data provided by isotopes.

The goal of this thesis is therefore to provide data derived from the Scandinavian snowpack in order to improve the understanding of the land surface signatures in relation to the atmospheric dynamic. Explicitly, the thesis seeks to know how far the stable water isotopes can provide information about a given winter and compare these results to the winter of 2010.

B. Theoretical basis

As we will deal a lot with isotopes in this thesis, it is helpful to remember the theoretical basis regarding the isotopic signal of precipitations and also exhibit some of the central concepts about North Atlantic Oscillation which influences the climate dynamic in the northern Europe.

1. Stable Water Isotopes

1.I. Notations

The water molecule is hydrogen and oxygen. Several isotopes exist for these two elements, the most abundant are ^{1}H and ^{16}O for hydrogen and oxygen (more than 99%). The other isotopes we are interested in are ^{2}H (D for Deuterium) and ^{18}O whose abundance are respectively 0,015% and 0,2%. Among the six possible combinations, only $^{1}H^{2}H^{16}O$ and $^{1}H_2{}^{18}O$ are measured because low abundance of the remaining isotopes. The composition of isotopes is analyzed using the delta notation δ using a standard :

$$\delta_{18_O} = \frac{\left(\frac{H_2{}^{18}O}{H_2O}\right)_{sample} - \left(\frac{H_2{}^{18}O}{H_2O}\right)_{standard}}{\left(\frac{H_2{}^{18}O}{H_2O}\right)_{standard}} * 10^3$$

Equation 1 : $\delta^{18}O$ equation

All the results are given against the same standard for every laboratory in the world, that is the SMOW (Standard Mean Ocean Water), defining $\delta_{D\text{-}SMOW}$ as 0‰ and $\delta^{18}{}_{O\text{-}SMOW}$ as 0‰. This enables to compare results across the globe and is necessary for the calibration for standardized analysis.

1.II. Isotope fractionation

The water can have different δ_D and $\delta^{18}{}_O$ values. The range amounts to about 400 ‰ for δ_D and 40 ‰ for $\delta^{18}{}_O$. These differences are due to a phenomenon called isotope fractionation. Indeed, isotopes react differently to a transformation of water phase. This explains the variability between isotope composition of water masses. For example, heavier water molecules as $HD^{16}O$ or $H_2{}^{18}O$ have a lower mobility because of their higher masses. The Boltzmann equation can be used to easily explains this fractionation effect as :

$$kT = \frac{1}{2}mv^2$$

K : Boltzman constant ; T : temperature ; m : mass of molecule ; v : average molecular velocity

Equation 2 : Boltzmann equation

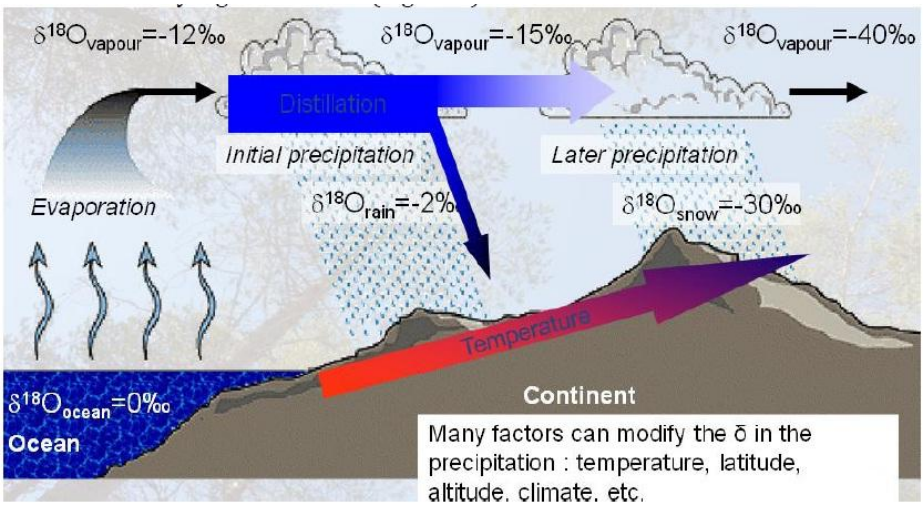

Figure 1 : Stable isotope and water cycle.

The kinematic energy associated with isotopic fractionation is solely a function of temperature. So if kT is constant for given water mass, the molecules with higher masses have a smaller velocity. That is why during evaporation, water vapor has lower δ_D and δ^{18}_O than the remaining liquid vapor. The lighter water molecules evaporate more easily. For precipitation phenomenon, the heavier water molecules condense more easily (figure 1).

This kinematic model explains the continental effect seen in precipitation : The further a cloud comes from the evaporating area (typically the ocean), the lower are the δ_D and δ^{18}_O of the vapor. This continues for additional precipitations if we assume that there is no mixing with other air masses leading to a rain-out of stable water isotopes as clouds move in land (figure 1).

2. North Atlantic Oscillation

The weather pattern in the North of Europe is partly determined by the atmospheric pressure difference between Iceland and the Acores. There is an index based on this difference called North Atlantic Oscillation index (NAOi). It can be positive or negative. When it is positive, European winter is warm and wet because air masses mainly come from the Atlantic Ocean. This is due to the difference between the pressures over the pole and the ones over the Acores being quite low. Whereas when it is negative, European winter is dry and cold because air masses come from Siberia and more generally the north of Russia. In that case, the pressures over the pole are anomalously high while they are lower over mid-latitudes (figure 2.a). For example, the geopotential height at 500mb anomaly averaged over winter 2010 corresponds to a negative phase of the NAOi (Thompson and Wallace ,1998). Moreover NAOi over winter 2010 was extremely negative (figure 2.b) (Cattiaux et al., 2010) as well as winter 2011.

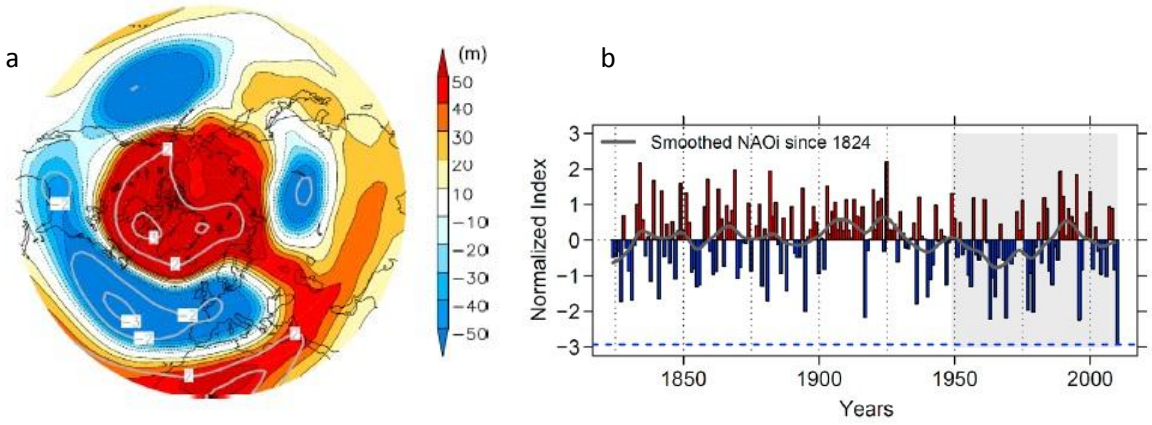

Figure 2 : Geopotential height at 500mb (Z500)anomaly averaged over winter 2010 (a). Normalized 1824-2010 time series (bars) constructed as the difference in sea level pressure between Lisbon, Portugal and Stykkisholmur, Reykjavik, Iceland. The mean winter sea level pressure data at each station was normalized by division of each seasonal pressure by the long term mean standard deviation. The spline-smoothing of NAOi is represented bu the grey bold line, it removes fluctuations with periods less than 4 years. Winter 2010 is indicated by the blue dashed line (b). (Cattiaux et al., 2010).

3.SWI in the snowpack

Analyzing the snowpack enables the study of the precipitations occurring during the course of winter. This enables to work on climate dynamics and forms the main motivation for this current research thesis.

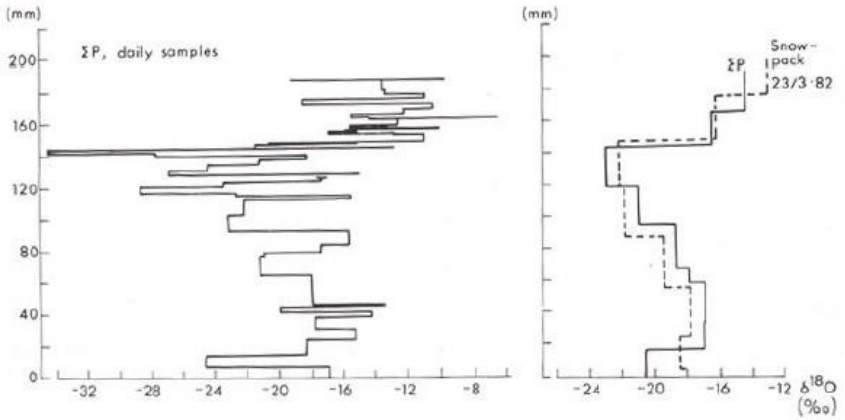

Vertical axes : water equivalent in mm ; horizontal axes : δ^{18}_{O} en ‰.

Figure 3 : δ^{18}_{O} layering of the snowpack compared to the δ^{18}_{O} of winter precipitations. (Rhode, 1987).

In 1987, Rhode plotted the isotopic composition of the precipitations and the snowpack in central Sweden (figure 3). His study reveals that a snowpack records the isotopic composition of the precipitations over the winter. Obviously the snowpack has to be undisturbed over the winter : the temperature has to stay below 0°C to avoid melting, the snowpack has to be in an open air area to avoid any snow drift development and finally, the snow has to not be mixed (Rhode, 1987).

C. Site description

1. Geography

The investigation took place in early March from the 4th until the 12th mainly in the north of Sweden between the latitudes 62° N and 68° N. In addition, a few cores were collected in Norway, in Trondheim and in Mo I Rana. The study area is delimited on the West by the Norwegian Sea and on the East by the Baltic Sea. The most southern sample sites are Sveg and Härnösand and most northern is Abisko (figure 4).

Scandinavia has a mountain chain, Skanderna, that is oriented NNE-SSW on the boundary between Norway and Sweden. This mountain chain is part of the Caledonian chain formed at the Paleozoic era. The highest mount is situated in Norway, Galdhøpiggen, and reaches 2 469 m above sea level. Besides this mountain chain, topography of Sweden is relatively flat. According to G. Rousseau, 2010, the East-West average gradient from the mountains to the Baltic sea is 0,0023 m/m. Its flatness can be explain by the age of the Baltic shield that is mostly of Archean and Proterozoic gneisses and greenstones (A. Slabunov, 1999) that has been eroded by successive Pleistocene glaciations. Concerning the vegetation in this part of Fennoscandia, it is mainly composed of spruces and pines.

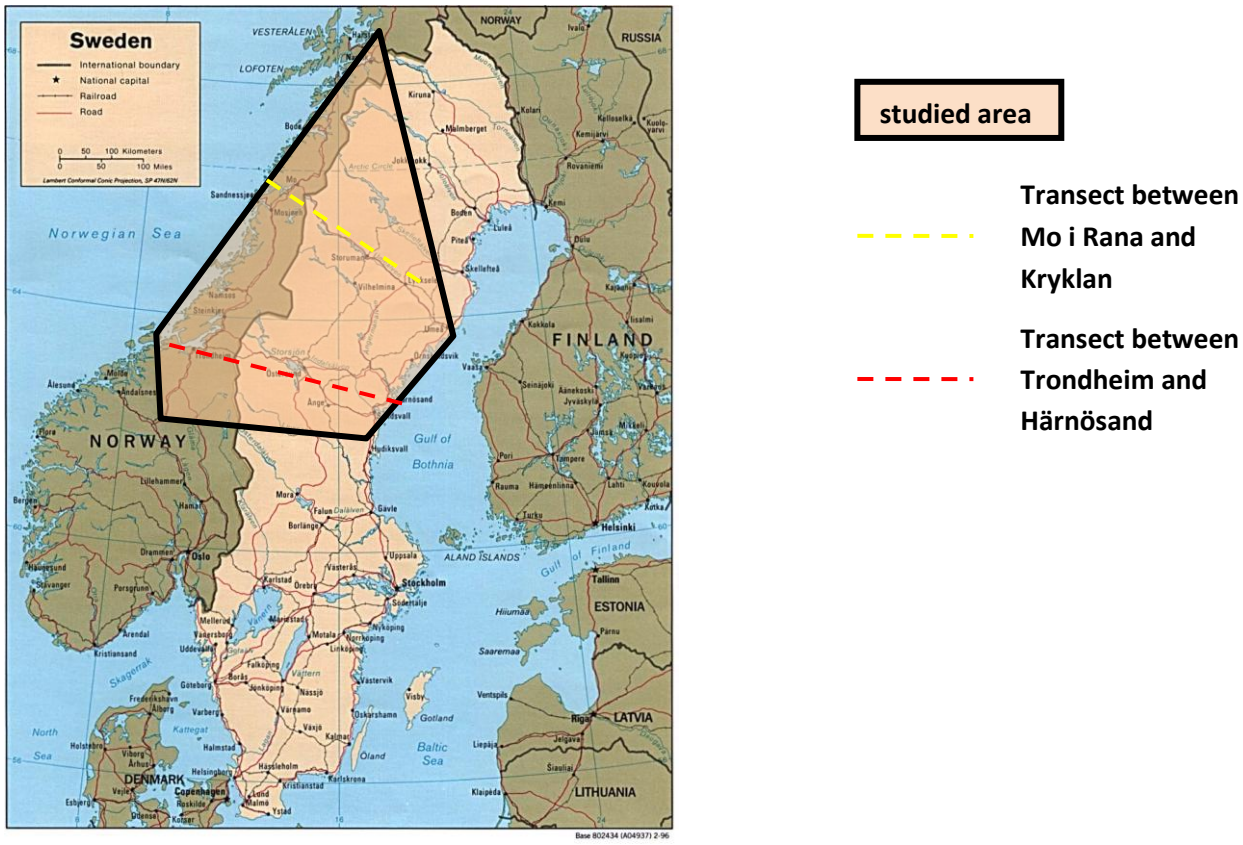

Figure 4 : Location of the studied area in Scandinavia.

2. Climate

Scandinavian climate (figure 5) is mostly influenced by the high latitude that induces a contrasted seasonality and a daytime varying from 0 hour in winter to 24h in summer for parts above the Arctic Circle in northern Sweden.

Though, Scandinavia has quite a temperate climate because of the warm oceanic streams going along Europe as Gulf Stream and induces a higher temperature than other places at same latitude across the Globe. Sweden receives on average 554mm of precipitation annually (a bit less than France's 619mm).

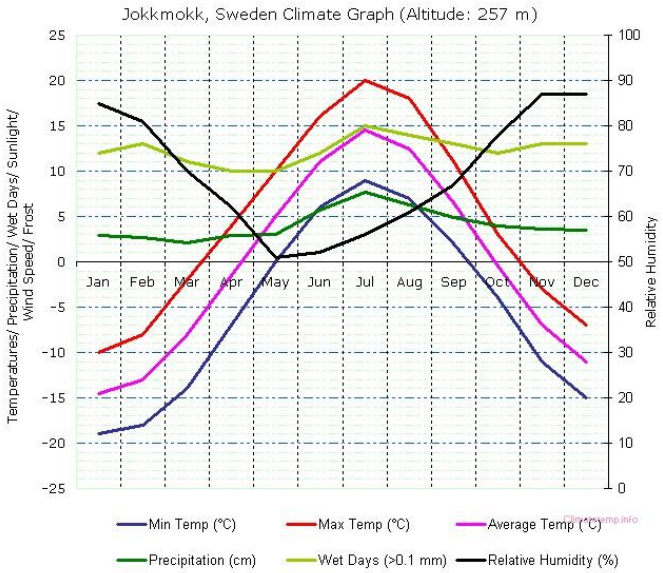

Figure 5 : Jokkmokk (66°36'N 19°51'E, alt. 257m) climate graph.
Source : www.climatetemp.info

The North Atlantic Oscillation is a parameter that influences climate dynamic over North of Europe and therefore largely influences Swedish climate. As it is explained in the review of literature, the NAO index was extremely negative during winter 2009-2010(figure 2, b).

3. Winter 2010-2011 in Sweden

3.I. NAO index

Basically, the negative phase has dominated the circulation for almost ten years and the NAOi tends to get stronger since winter 2010 (figure 7). In addition, the mean calculated for the three months DJF is about -0,68 for this winter 2011 whereas last winter, it was almost -1,67 (calculated from the monthly data given by the Climate Prediction Center). The procedure used to calculate the NAO teleconnection is based on a technique called rotated principal component analysis (RPCA) (see Barnston and Livezey, 1987, for more details on this technique). This RPCA technique is applied to monthly mean standardized 500-mb height anomalies obtained from the Climate Data Assimilation System (CDAS) in the analysis region 20°N-90°N between January 1950 and December 2000. The anomalies are standardized by this 50 years base period monthly means and standard deviations. We will see how the NAO can be illustrated into the isotopic composition of snow pack for this winter and link it to the climate dynamics.

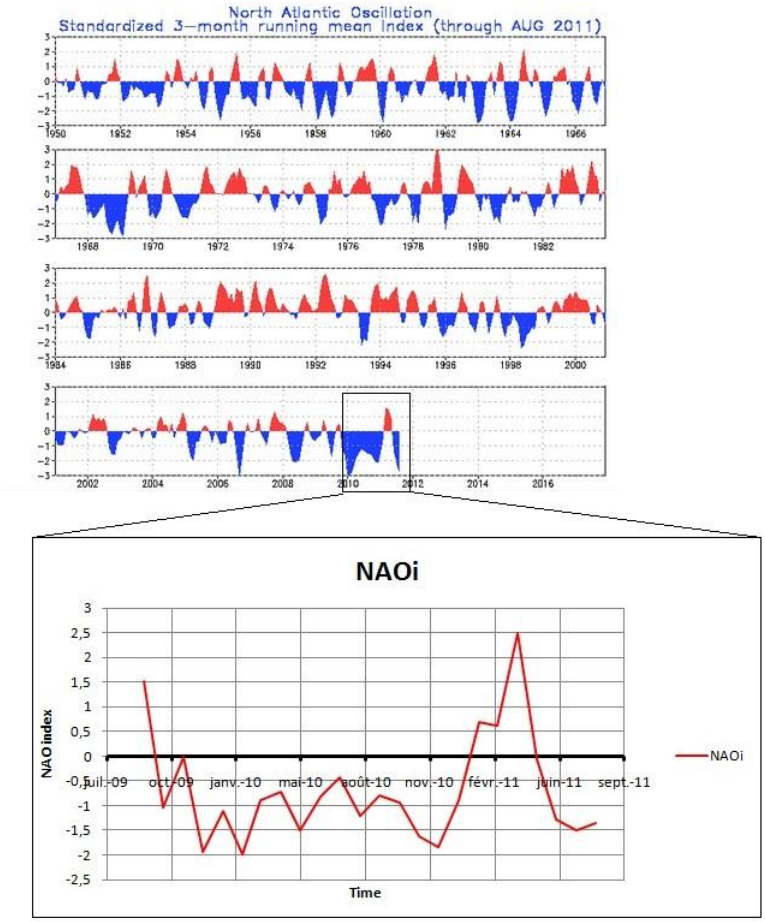

Figure 6 : Daily NAO index for the period 12th of October 2010 – 8th of February 2011. Each daily value has been standardized by the standard deviation of the monthly NAO index from 1950 to 2000 interpolated in the day in question. North Atlantic index time series from 1950 to 2011: standardized 3-months running mean NAO index. (Climate Prediction Center, http://www.cpc.ncep.noaa.gov)

3.II. Snow depth

Winter 2009-2010 in Sweden was characterized by an unusual snowfall amount and low temperature (G. Rousseau, 2010). Actually, winter 2010-2011 was even snowier than the prvious (figure 7). The snow pack was more than 50cm thick over the whole studied area on the 15th of March 2011 according to the observations made by Sweden's Service Meteorological and Hydrological Institute.

Figure 7 : Snow depths recorded over Sweden the 15/03/11 (Service Meteorological and hydrological Institute, www.smhi.se)

3.III.Temperature in Sweden

The evolution of the temperature from October to March in Sveg shows that the seasonality is not the only parameter governing the temperature variability. Indeed, while the temperature is rising during January, we can observe a big drop in February, and then the temperature rises again.

The other temperature profiles over Sweden, in Östersund(63,2°N 14,6°E, center of the studied area), in Kiruna (67,8°N 20,3°E, north of the studied area) and Härnösand (62,7°N 17,8°E, south-east of the studied area) from the 10th of November 2010 to the 4th of April 2011 reveal the same evolution during these months, with a quick decrease of the temperature during February (annex 4). This cold event is therefore expanded all over Sweden.

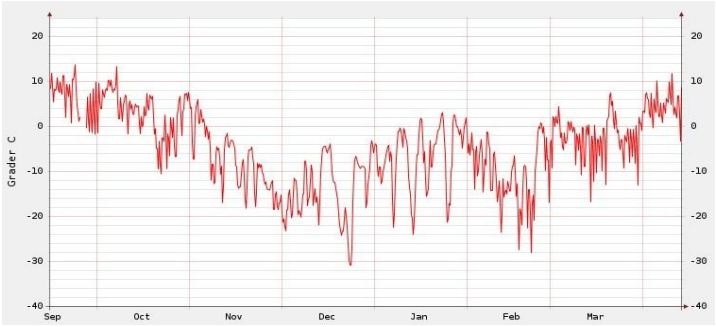

Figure 8 : temperature recorded in Sveg which is the more Southern city of the studied area from September 2010 until March 2011).(www.temperatur.nu).

As we can see on figure 8, the temperature in the south of the studied area exceeded rarely 0°C. We can thus assume that the snow pack did not melt until the end of the sampling campaign. Any melting could have potentially induced fractionation and a mixing of the isotopic composition within the snowpack because of the percolation of water into the snow. Since melting was unlikely during the period of sampling, there were good conditions to carry out this project and sample undisturbed snow cores.

D. Field Trip

1. Determination of the sample sites

Figure 9 : final itinerary in the northern half of Sweden. The "S"'s stand for the sample sites we stopped in.

The field trip was done with support from A. Peralta Tapia, a PhD student from Umeå University whose studies focus on the catchment of Kryklan near Umeå under the supervision of H. Laudon. The sites we planned to stop at were Abisko (68,355°N 18,803°N) in the north of Sweden, which is a well studied catchment by S. Lyon and Kryklan (64,282°N 19,812°E), near Umeå. We also collected snow cores on the same transect as G. Rousseau from 2010 at the latitude 63,5°+/1° between Trondheim and Sundsvall. In addition, a second transect oriented NW-SE was performed more in the North, between Mo I Rana (66,323°N 14,237°E) and Krycklan. The other sampling sites were selected to have the most homogeneous dataset possible since they all are close to weather stations (less than 10km) which record meteorological paramaters like temperatures, precipitations or wind speed.

Finally the sampling campaign took place at the beginning of March, between the 4th and the 12th, before the first positive temperatures in order to avoid any evaporation or melting and almost after the last snowfalls. The studied area covers a 350.000km² surface, between 62 and 68°N and 10 and 21°E (figure 9) representing a trip which is 3500km long.

2. Method of sampling

Two different types of core were collected. Total cores were collected thanks to a 1 m long 4,8cm thick pipe (figure 11) to study the spatial variability of isotopic composition in the winter snowpack between sampling site. Other cores were sampled thanks to a Russian Corer usually used for sampling lake sediments. However, based on previous work and experience, this corer worked well for snow and kept cores intact. Those cores sampled with the sample corer were cut into 2.5cm slices in order to study the temporal variability of

isotopic signature in each site. Near those cores, some additional cores were sampled few meters or kilometers away and cut into 5cm slice in order to validate the high resolution cores. The Russian Corer makes semi-circle cores with a 5cm radius and is limited in height to 150cm (the snow pack never exceeds 150cm in this study) (figure 10).

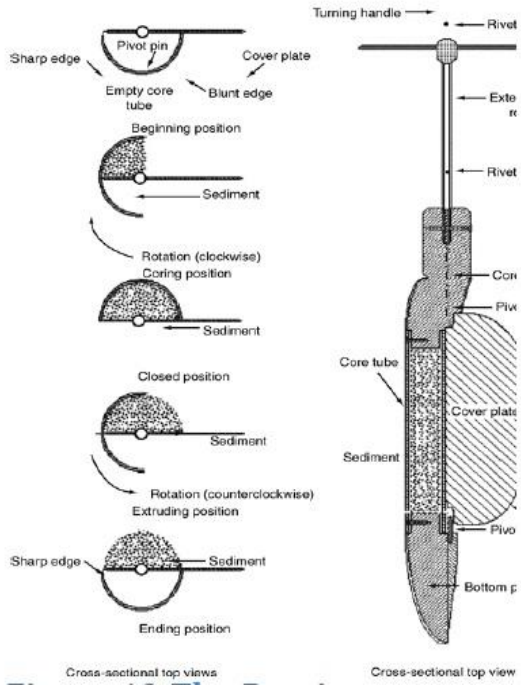

Figure 10 : The Russian Corer, used to collect the snow cores

Even if we tried to sample every site with the same protocol, some sites were not sampled with this protocol. The first reason is that due to logistic constraints we had to make the 3500km loop in 9 days and we were running low on time.

Also, when the snowpack was very thick, we samples only low resolution cores, i.e. 5cm slices.

In total, 95 snow cores were collected : 21 high resolution cores, 26 low resolution cores and 48 total cores. These 766 samples were kept during the transportation in sealed freezer bags. The samples were weighed the sampling day (figure 12).

The samples were brought back to Stockholm University in order to be analyzed with LGR-LS. They were stored in a freezer to avoid any melting, leakage or mixing. The samples were removed from the freezer 3 days before the preparation of vials in a refrigerator. The samples were weighed again before analyzing in order to check for any leakage that might have occurred during the transport.

Figure 11 : Sampling total cores with the pipe

place	day	number of high resolution cores	number of low resolution cores	number of total cores	number of cores	coordinates
Stockholm	11/02/2011	1	0	1	2	N 59,369 E 18,065
Stockholm	02/03/2011	1	0	1	2	N 59,369 E 18,065
Härnösand	04/03/2011	1	1	1	3	N 62,667 E 17,817
Sveg	04/03/2011	0	0	1	1	N 62,041 E 14,689
Sveg	05/03/2011	1	2	1	4	N 62,088 E 14,248
Tännäs	05/03/2011	1	1	1	3	N 62,441 E 12,616
Trondheim	05/03/2011	1	1	2	4	N 63,3246 E 10,3208
Stor Ulvan	06/03/2011	1	1	1	3	N 63,166 E 12,336
Mörsil	06/03/2011	1	2	2	5	N 63,3089 E 13,7125
Östersund	06/03/2011	1	1	2	4	N 63,202 E 14,640
Hallaxasen	07/03/2011	1	2	3	6	N 63,764 E 15,346
Laxbacken	07/03/2011	1	1	2	4	N 64,642 E 16,479
Blaiken	08/03/2011	1	1	2	4	N 65,246 E 16,890
Nordanas	08/03/2011	1	2	3	6	N 65,460 E 16,085
Hemavan	08/03/2011	1	1	1	3	N 65,771 E 15,112
Mo i Rana	09/03/2011	1	1	2	4	N 66,323 E 14,237
Abisko	10/03/2011	2	4	5	11	N 68,355 E 18,803
Kiruna	10/03/2011	0	1	1	2	N 67,846 E 20,340
Jokkmokk	11/03/2011	1	1	2	4	N 66,566 E 19,789
Arvidsjaur	11/03/2011	1	1	2	4	N 65,619 E 19,128
Krycklan	12/03/2011	2	2	12	16	N 64,282 E 19,812
total	after 9 days	21	26	48	95	

Figure 12 : Summary table of all the cores collected during the field trip in 2011

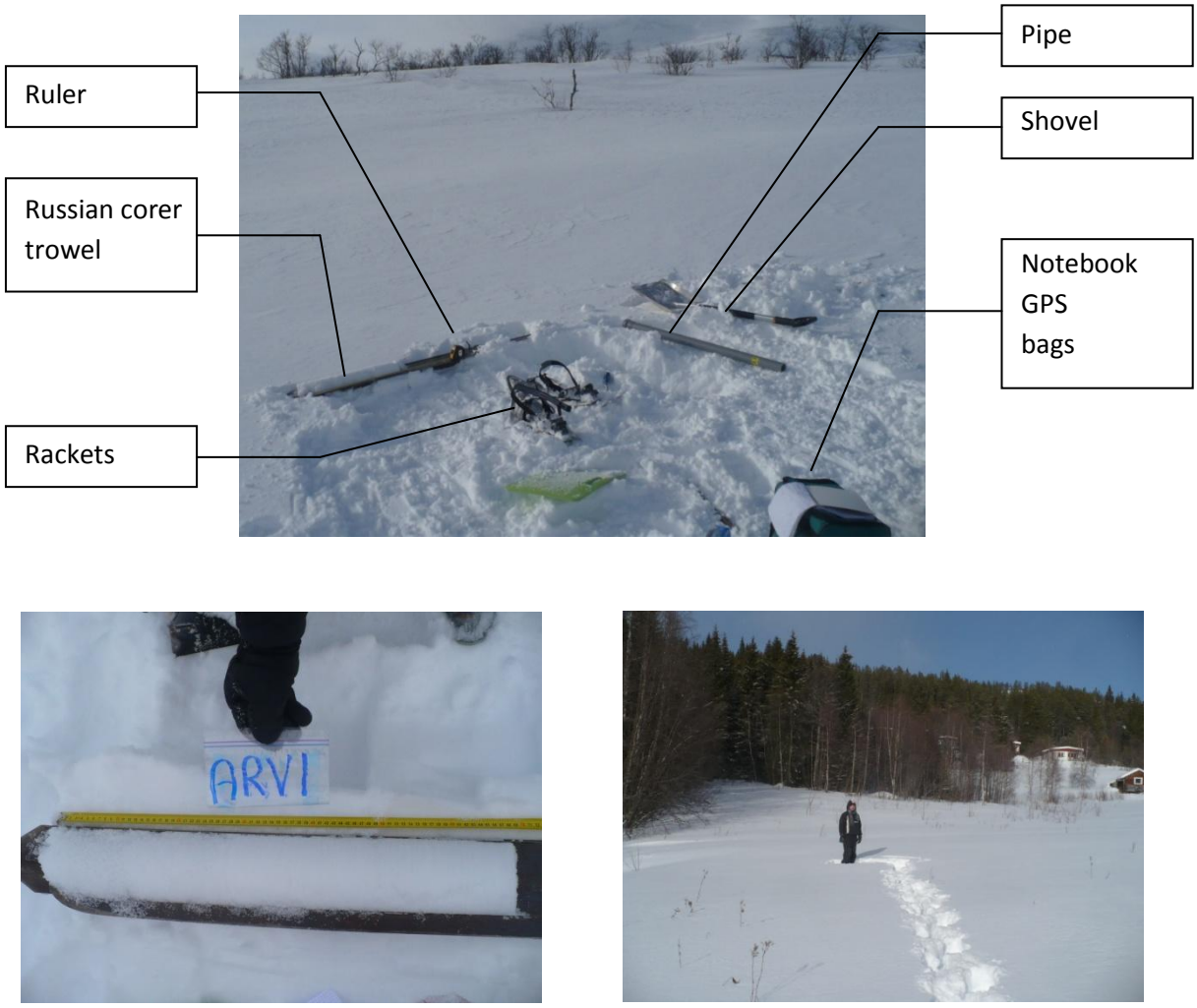

Figure 13 : Top picture : sampling site with the different tools used. Bottom left : picture of snow core with its reference (performed for each core). Bottom right : picture of the global site in order to explain potential particularities of the measurement by elements of the sampling site (performed for each site)

To summarize, at the end of each day, all the samples were weighed. For each site, one high resolution, at least one low resolution and several total cores were collected. The coordinates for each sampling site were measured by the GPS. A picture of the site was taken and observations about the site noted. On each core, the length/depth was measured with the ruler, a picture of the entire core with the ruler was taken and the observations about the core were noted (e.g., the grain size, the presence of ice layers or rain marks at the surface) (figure 13).

3. Variables and accuracy

3.I. Direct measure

a. **length** : the length of each core has been measured thanks to a simple ruler whose precision is 0,001m. This ruler was used to measure the total bulk cores and also to high

resolution cores that were cut with the trowel. Since this trowel cut both top and bottom of a sample, the error was therefore for multiplied by 2 for the slices because the slices

b. **Global Position Satellite (GPS)** : the coordinates of each core is measured in situ thanks to a GPS Garmin 12 channel (reference number : 36401900), Garmin Olathe, Kansas, USA. The precision of this GPS is ±0,004° in latitude and longitude, i.e. if we consider earth as a sphere with a 6371km radius, there is an accuracy of ±167m along the longitude for the most northern part of the field area and ±209m for the most southern part. Along the latitude, it is almost ±445m.

c. **altitude :** the altitude of each core is measured afterward on Google earth where there is an accuracy of ±15m.

d. **Weight :** each sample is weighed as soon as possible (on the evening of the sampling day) in order to get the weight before any potential leakage during the transfer by car. The balance used during this field trip has a precision of 0,001g.

3.II. Calculated measures

a. **Volume** : the volume of each core is calculated with the equation of a semi-cylinder :

$$V_{russian\ corer} = \frac{L\pi R_{russian\ corer}{}^2}{2} \qquad V_{total\ core} = L\pi R_{total\ core}{}^2$$

Equation : volume of the cores collected with the Russian corer and volume of those collected with the pipe

The accuracy for the volume is dV/V = dL/L + 2dR/R, given the accuracy of the length measuring. The radius of the Russian corer is measured as 0,05m±0,001m. Also, we assume that there is an accuracy of ±0,001m when cutting the core with the trowel that is 0,001m thick. Therefore, the volume of 2,5cm slice is 98cm^3±11cm^3 and for a 5cm slice, it is 196cm^3±15cm^3.

b. **density** : the density is calculated with the equation :

$$density = \frac{weight}{volume}$$

Equation : density equation

The accuracy for the calculated density is dd/d = dW/W + dL/L + 2dR/R. The density is therefore estimated at about ±0,02g/cm^3.

E. Material and Methods for the isotopic analyzes

1. Material

1.I. Samples and standards preparations

To prepare samples for analysis in the LGR-LS, all the samples were prepared in ND832.11,6mm screw neck 1,5ml vials with a PTFE/silicone/PTFE septum. The LGR-LS notice says that the vials must be filled with a volume between 0,5ml and 1,5ml but when the first analyzes were run, there were some droplets at the top of the vials. This means that there was some evaporation and condensation in the vial because the lab temperature was too high. Therefore, the vials were filled as much as possible, with 1,6ml, letting air space in the vial and avoiding any trouble of over pressure. Vials were filled with a 500µl pipette. As such, it is likely that the accuracy of the volume in each vial has no influence on the measurement.

The same vials and pipette were used to prepare all the internal standards required by the LGR-LS machine.

The standards that we used were internally prepared standards because, on one hand, this is less expensive than obtaining IAEA standards like SMOW, SLAP or GISP and on the other hand the isotopic composition can be set closer to those expected by the collected samples. The internal standards we used were tap water and ice water, a third standard which was half of each. These provided adequate calibration.

We did not have enough vials to prepare all the samples at one time. Therefore, we had to wait the end of three days analysis, clean the vials with tape water (at least 3 rinses) and put them in the oven, temperature 60°C in order to avoid any pollution between samples and/or standard.

1.II. Laser spectrometer (LGR-LS)

Cavity ringdown laser spectrometry has been commercially available for less than 4 years and represents a potential leap in progress for stable water isotopes analysis in liquid water samples.

We have used a laser spectrometer to analyze all the isotopic compositions of water sample. This LGR-LS was developed by Los Gatos Research Inc. and the model used for our analysis was the DLT-100, delivered to Stockholm University in January 2010. The LGR-LS is based on the off-axis integrated cavity output spectroscopy (Off Axis ICOS) method that uses Beer's law relating the absorption to the isotopic composition of the water sample :

$$\frac{I_\nu}{I_0} = e^{-SL\chi P\phi_\nu} \quad \leftrightarrow \quad \chi = \frac{1}{SPL}\int ln\frac{I_0}{I_\nu}d\nu$$

Equation 5 : Beer's law, used by the LGR-LS

I_ν : *transmitted laser of frequency* ν ; I_0 : *initial intensity* ; S : *absorption line strength* ; ϕ_ν : *transition line shape function* ; L : *optical path length* ; χ : *mixing ratio* ; P : *gas pressure*

The chamber where the analyze occurs is composed by several mirrors that reflect a laser beam and so creates an artificial 3000m laser that crosses the water vapor. This long laser is necessary to get a good accuracy of the measurements (0,6‰ for δD and 0,2‰ for $\delta^{18}O$ according to the manufacturer's specification (Los Gatos Research inc., 2008).

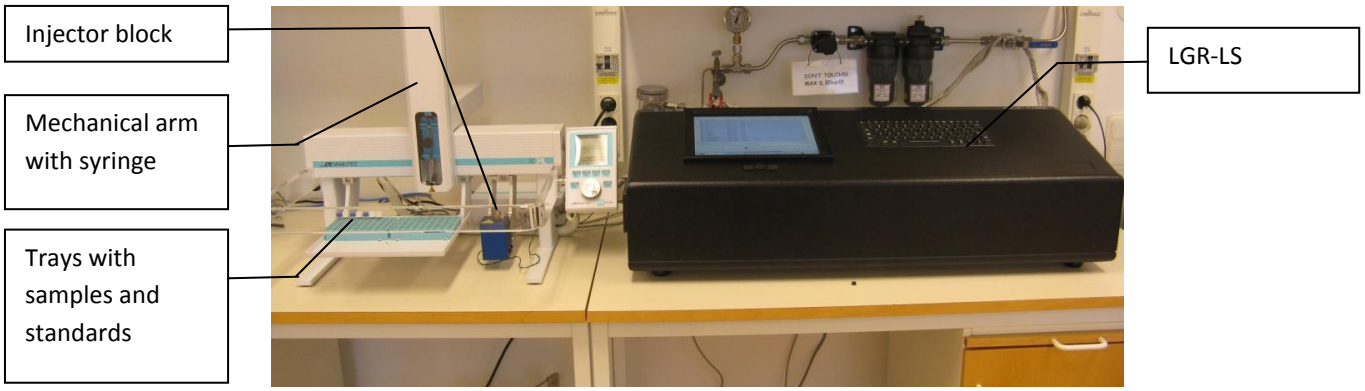

Figure 14 : Photography of the Laser spectrometer with the auto-sampler

The Laser Spectrometer is able to measure simultaneously the δD and $\delta^{18}O$, that reduces analyzing time. In total, analyzing and operational time is halved compared to the mass- spectrometer.

An auto sampler was also used. This sampler is composed of a mechanical arm with a syringe that samples 1µl off each vial (model 26-P/-mm/AS, 7701.2 NCTC) and 4 trays on which we can put 54 vials (figure 14).

2. Troubles with LGR-LS

When the Laser Spectrometer was delivered in January 2010, the manufacturer did not provide any procedure to follow to analyze the samples. Initial evaluation of the LGR-LS revealed severe issues with machine drift, memory effect and calibration affecting the accuracy and precision of measurements. Some statistical studies were done last year in order to estimate the error margin associated to the LGR-LS (C. STURM, 2010). This year, we had some trouble with the maintenance of the LGR-LS. I will first exhibit the technical

problems we had with the LGR-LS and explain how these were solved them. Then I will show the progress that was made last year and I will explain how this current study improves upon the protocol and post-processing analysis.

2.I. Technical troubles/maintenance

There were some troubles during the first uses of the LGR-LS in March dealing with the maintenance of the machine. Indeed, after one or two days of analyzing, some trouble flag appeared near the values making them unusable. The troubles flags (figure 15) which appeared were “dens”, “pres” and “oiso” that mean that the quantity of vapor reaching the cavity is too low or too high or too unstable to make an optimal measurement. Those troubles flags kept appearing even if the suggested maintenance was executed. Therefore we tried many runs with changing or cleaning one element of the transfer system between the LGR-LS and the vials in order to know from which part the trouble flag was coming from.

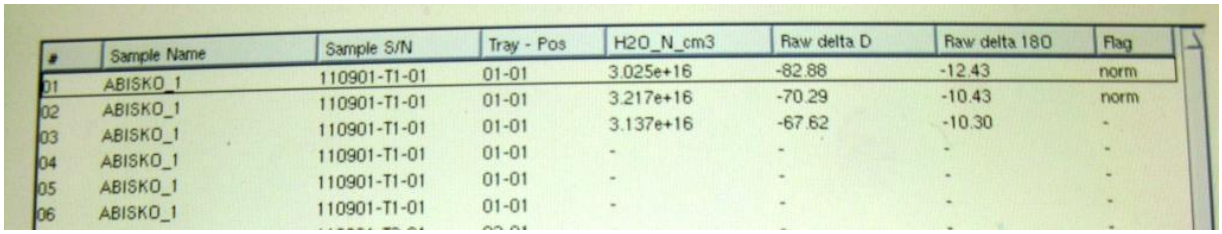

#	Sample Name	Sample S/N	Tray - Pos	H2O_N_cm3	Raw delta D	Raw delta 18O	Flag
01	ABISKO_1	110901-T1-01	01-01	3.025e+16	-82.88	-12.43	norm
02	ABISKO_1	110901-T1-01	01-01	3.217e+16	-70.29	-10.43	norm
03	ABISKO_1	110901-T1-01	01-01	3.137e+16	-67.62	-10.30	-
04	ABISKO_1	110901-T1-01	01-01	-	-	-	-
05	ABISKO_1	110901-T1-01	01-01	-	-	-	-
06	ABISKO_1	110901-T1-01	01-01	-	-	-	-

Figure 15 : Screen of the LGR-LS during running of the analyses

Those investigations revealed that some pieces of septa (silicone joint in the injector block which serves to prevent leakages of vapor) could stay stuck in the injector block and also in the transfer line. To avoid any trouble flag, the septum needed to be changed every day (about every 600 injections) and the transfer line has to be cleaned every three days (by unscrewing the line on the LGR and also on the injector block, putting dry air on both side of the transfer line and also on both side of the injector block). The syringe can also be stuck after several days of use. Therefore, it is necessary to verify if the syringe slips well enough to sample the good amount of water. The absorption spectrum during the analyses should show absorption on the order of 5 – 60% and the large, central peak near -1GHz should be roughly centered in the shaded grey box (figure 16).

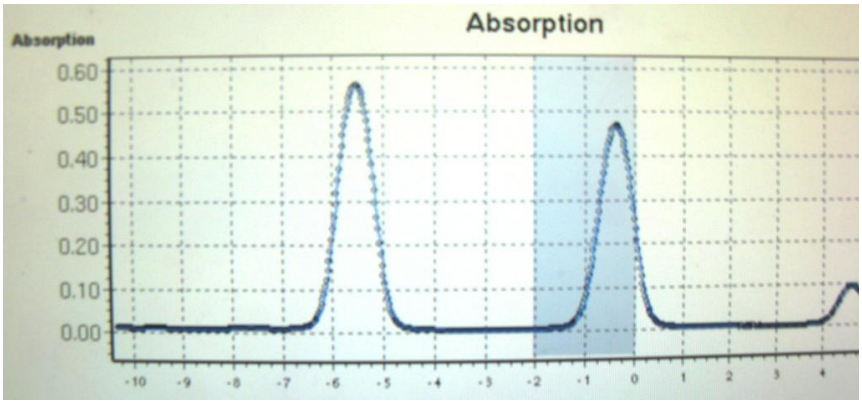

Figure 16 : Absorption spectrum with the shifted central peak in the shaded grey box

2.II. Memory effect

As the syringe is the same for all injections, it is responsible of pollution of a sample from the previous one. Indeed, after one injection, some droplets are still in the syringe and are mixed with the following sample. That is why several injections to analyze a sample are necessary; the first ones are not taken into account (considered too affected by the memory effect). The more injections are done, the less polluted are the last injections.

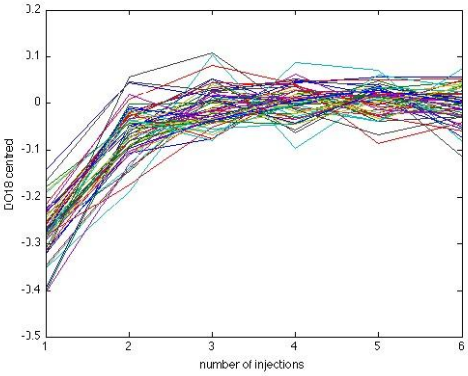

Figure 17 : Evolution of the $\delta^{18}O$ of the same standard LG2 ($\delta 18O$ = -15,55‰) analyzed 50 times after the analyze of LG1(-19,57‰).

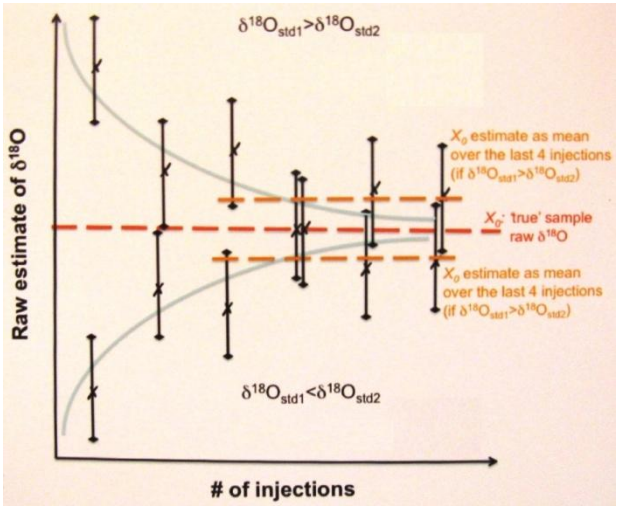

Figure 18 : Evolution of the $\delta 18O$ of the same standard LG2 ($\delta 18O$ = -15,55‰) analyzed 50 times after the analyze of LG1(-19,57‰).

G. Rousseau, last year, quantified this memory effect in analyzing 50 times the same two standards of known $\delta^{18}O$ with 6 injections (figure17). A statistical study of this dataset revealed that the pollution appears until the third injection and that the interval between the average expectancy on the four last injections and the theoretical value is 0,004‰ due to the memory effect. This interval is less than the variance of normal distribution on the last four injections and can be considered negligible.

An alternate method to estimate the true raw $\delta^{18}O$ of the sample and thereby minimizing the memory effect is to fit an exponential curve (figure 18) whose asymptote represents the unaffected raw $\delta^{18}O$. This method would improve both the accuracy and precision of the measurement.

$$X = X_0 \pm C \cdot e^{-\frac{t-t_0}{\tau}}$$

Equation 6 : fitting exponential curve
X_0 : true sample raw $\delta^{18}O$; C τ : parameter that represents the speed reaching the limit ; $X_0 \pm C$: initial value ; t : number of injection ; t_0 : first injection

G. Rousseau, after 70 runs, reported that no stable τ was found and therefore, an exponential curve had to be found for each evolution. Finally a simple average method was used to estimate the true raw $\delta^{18}O$ because it did not give significantly better results.

The memory effect has also an influence on the analysis of standards that are measured consecutively. So if the same standards are used during all the experiment, their isotopic composition will change non-negligibly.

2.III. Calibration

A calibration is necessary to calculate the real value of δD and $\delta^{18}O$ for samples. Indeed, the LGR-LS does not give directly the real value. There is a gap between the real value and the value calculated by the machine. That is why we need to measure standards of known value to quantify this gap and minimize bias due to this gap to calculate the real value of samples.

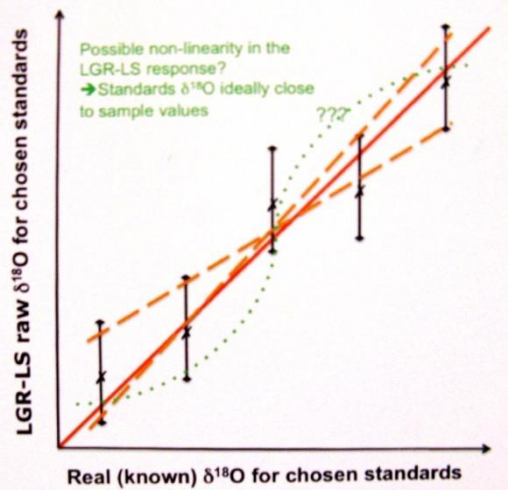

Figure 19 : calibration method. The computed regression is appliedto the neighbouring sample raw $\delta^{18}O$ values to obtain calibrated 'real' $\delta^{18}O$ measurements.(C. Sturm, 2010)

To calibrate the LGR-LS a regression line Based on the standards is computed. Though, there is a possible non-linearity in the LGR-LS response (figure). So there will be an effect from the choice of standards (number and $\delta^{18}O$ range of the chosen standards) on the measurements' precision and accuracy.

2.IV. Machine drift

The initial evaluation revealed also that the gap was not stable during time. If we calculate all the samples with a fixed initial gap, the following results will be biased. So the

standards have to be measured regularly to modify the calibration in function of the machine drift.

2.V. Injection duration

An injection lasts about 2 minutes. This parameter is important to take into account for the standard bracketing protocol. Indeed, the more injections there are, the less the memory effect affects the measurements but the more important is the machine drift. As such, some trade off needs to be considered.

2.VI. Statistical studies about error and Memory Effect

To develop the investigation about error and memory effect for this current study, 5 samples of known isotopic composition monotonically increasing equidistant $d^{18}O$ values were created (by mixing the 2 existing internal standards, tape water and ice water). We will dispose the 5 samples according to an order obtained from a simple Matlab script, to cover all possible combinations, for both increasing and decreasing pairs (figure 20).

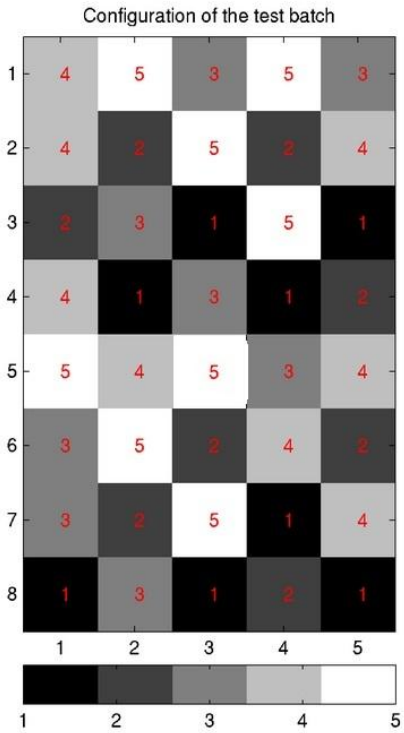

Figure 20 : configuration of the test batch to investigate the memory effect. The numbers stand for the different internal standards.

The five samples were all made by mixing the internal standards : tape water whose $\delta^{18}0$ is -8,28‰ recalled vin5 and ice water whose $\delta^{18}0$ is -30,86‰ recalled vin1 which were the two samples of extreme values. The mixing has to be very accurate so we use a very precise weighing machine (±0,001g). So the three other intermediates would have $\delta^{18}0_{vin2}$= -13,93‰ δD_{vin2}= -110,3‰ for vin2, $\delta^{18}0_{vin3}$=-19,57‰ and δD_{vin3}=-155,9‰ for vin3 and $\delta^{18}0_{vin4}$=-25,22‰ and δD_{vin4}= -199,12‰for vin4 and

Those five samples have been measured against the IAEA standards (International Atomic Energy Agency) with 12 injections (disregarding the first injections that are considered too affected) in order to avoid the memory effect on the calculation of the 'true' real $\delta^{18}0$ of those internal standards. The values of $\delta^{18}0$ calculated for the three intermediate standards are $\delta^{18}0_{vin2}$ = -13,79‰ and δD_{vin2} = -109,37‰ for vin2, $\delta^{18}0_{vin3}$=-19,54‰ and δD_{vin3} = -155,3‰ for vin3 and $\delta^{18}0_{vin4}$=-25,20‰ and δD_{vin4}= -199,36‰ for vin4. So they are very close to the expected values and can be used in the test batch for the statistical investigation.

We chose to measure standards every 5 samples to correct the machine drift. This test batch was run 6 times. For the first two runs, the samples were analyzed with the IAEA standards firstly with 6 injections and then 9 injections. For the second two runs, the samples are analyzed with vin1, vin3 and vin5 (used as standards), firstly with 6 injections and then with 9 injections. For the last two runs, the samples are analyzed with themselves as standards (vin1, vin2, vin3, vin4 and vin5).

The evaluation of the error for each of these test batches revealed that the batch analyzed with vin1, vin3 and vin5 with a standard deviation of 0,2‰ for $\delta^{18}O$ and 1,8‰ for δD that were the lowest.

3. Our analyses

Finally, it has been chosen to make 6 injections to analyze all the samples because of the duration of an injection (2 min) and also because the more injections there are, the more important is the machine drift. We have used 3 internal standards, vin1 ($\delta^{18}O$ = -8,74‰ and δD = -66,85‰), vin3 ($\delta^{18}O$ = -19,29‰ and δD = -152,12‰)and vin5 (($\delta^{18}O$ = -29,78‰ and δD = -237,15) which were measured every 5 samples (figure 21). Each standard were used just once to avoid any use of polluted standards. The LGR-LS cannot be programmed for this sample-standard configuration so the standards have to be measured as 'samples' in the configuration screen. For this batch configuration, we managed to measure 60 samples every day. Therefore, the standards had to be measured 13 times that represents 39 standard measurements (13 of each standard). The run represents 594 injections (6 inj.*60 samp.*2min.+6inj.*39stds.*2min.) that represent a duration of 19 hours.

VIN1	VIN3	VIN5	S1	S2	S3	S4	S5	VIN1'	VIN3'	VIN5'	S6	…

…	$VIN1^{(12)}$	$VIN3^{(12)}$	$VIN5^{(12)}$	S56	S57	S58	S59	S60	$VIN1^{(13)}$	$VIN3^{(13)}$	$VIN5^{(13)}$

Figure 21 : configuration batch for all the samples. The standards are red and the samples are blue

We did not have enough time to create a program using the fitting of an exponential curve. We used an excel makro made by Magnus Mörth which enables the calculation of the average on the last four measurements. The makro corrects the machine drift and normalize the deltas against our internal standards.

4. Conclusion about the LGR-LS

A thorough statistical investigation of liquid stable water isotope samples by LGR-LS has been performed since it has been delivered at Stockholm's University. Though it is faster than the conventional mass-spectrometry, experimental protocol and post-processing procedure have still to be improved to insure that the measurement obtained by the LGR-LS achieve a similar accuracy and precision as mass spectrometry.

Nevertheless, the precision determined for this current study is acceptable to investigate environmental issues. As such, the remainder of this thesis will focus on the analysis and representation of the snow samples collected during the northern Sweden field campaign.

F. Results

1.Dataset

Here are a few statistical calculations to characterized the dataset resulting from the analysis of the snow samples collected during the field trip. The average for the $\delta^{18}O$ of those samples is **-18,35‰**, for the δD, the average is **-130,88‰**. The range for the $\delta^{18}O$ is **[-26,43;-6,03]** and **[-195,72;-37,87]** for δD. The standard deviation reaches **3,46‰** for $\delta^{18}O$ and **27,64‰** for δD. The standard deviation for δD is about 8 times the standard deviation of $\delta^{18}O$ because of their mass difference. The two histograms have the same shape because isotopes of hydrogen and isotopes of oxygen react the same during evaporation or precipitation (figure 22).

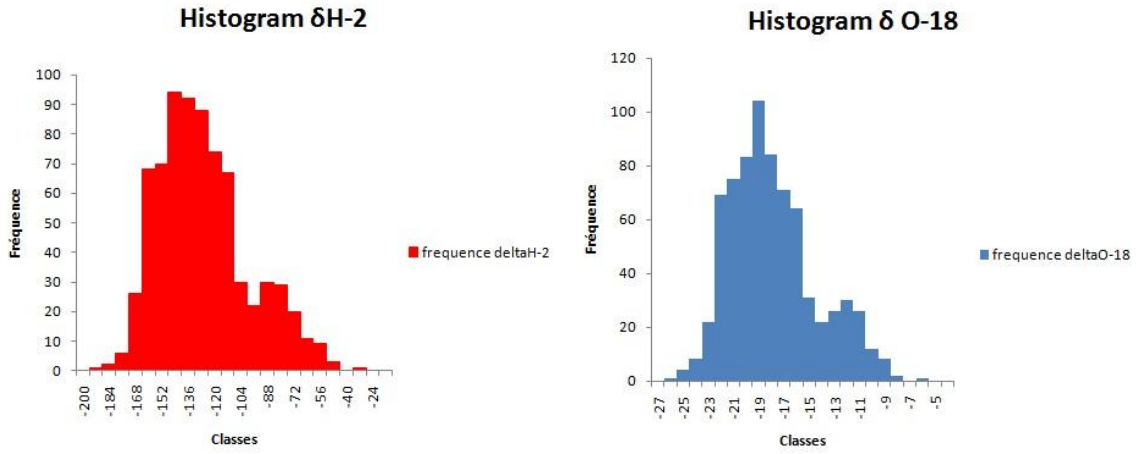

figure 22: histograms of the δD dataset (red) and of the $\delta^{18}O$ dataset (blue).

The Local Meteoric Water Line has been plotted to be compared to the Global Meteoric Water Line (GMWL) (figure 23) whose equation is $\delta D_{GMWL} = 8\delta^{18}O_{GMWL} + 10$. This LMWL has been plotted thanks to a linear regression of the dataset and its equation is $\delta D_{GMWL} = 7{,}8\delta^{18}O_{GMWL} + 12{,}6$. The two slopes are quiet similar (7,8 for LMWL versus 8 for GMWL) that enable us to assume that the snow falls have not been affected any evaporation or melting. Indeed, fractionation coefficients of δD and $\delta^{18}O$ have a ratio equal to 8 because (ratio between 18O and D masses). There is an additional kinetic fractionation for evaporation due to the different diffusivity of the two isotopes that moves the isotopic signal away from the GMWL (Clark and Frotz, 1997). The Deuterium excess is higher in the LMWL (12,6) than the GMLW (10). This deuterium excess depends on the evaporation degree and the origin of air mass. The deuterium excess in the GMLW is an average and there can be local and seasonal effect influencing this Deuterium excess. (J.R. Gat, 2000).

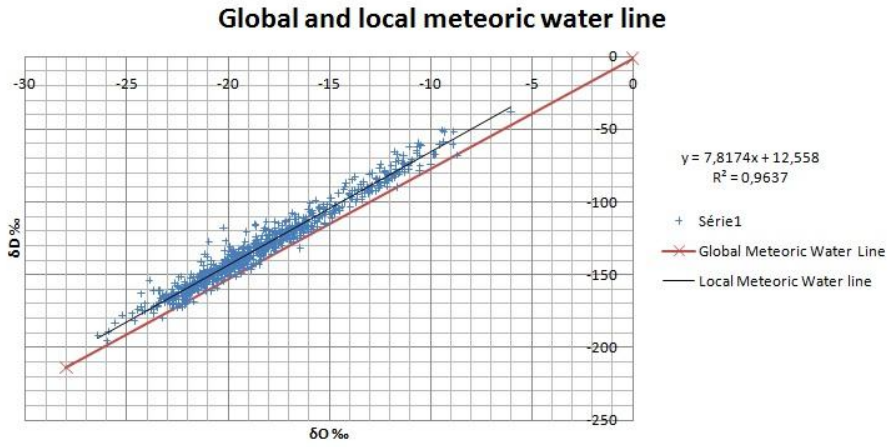

Figure 23 : Plot of the Local Meteoric Water Line thanks to a linear combination of δD and $\delta^{18}O$ of the snow samples collected during the field tripin March 2011 versus the Global Meteoric Water Line (Craig, 1961).

Comparisons between isotopic composition of cut cores and total cores have been done in order to check any bias between those two types of cores. The weighted mean of the cut cores is calculated with the following formulae :

$$\delta_{SWI,tot} = \frac{\sum_{n=top}^{bottom} \delta_{SWI,n} * Weight_n}{\sum_{n=top}^{bottom} Weight_n}$$

Equation : Weighted mean equation

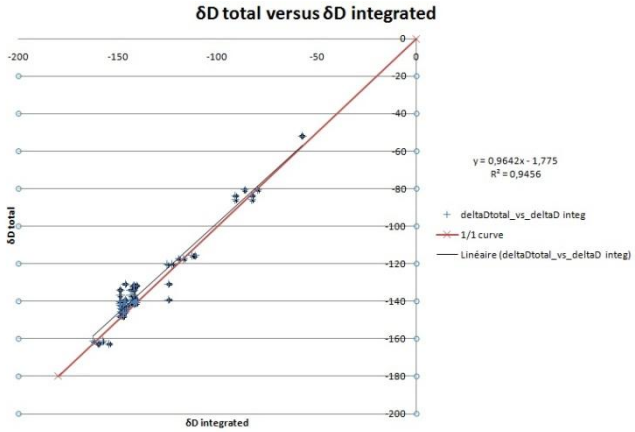

Figure 24 : $\delta^{18}O$ calculated on the total cores as functions of $\delta^{18}O$ calculated on cut cores, black bars represent errors.

The $\delta^{18}O$ calculated on the total core versus integrated on the cut cores are well aligned with the comparison bisectrice. This good correspondance proves that there is no biais from the method to collect total cores to the method to collect cut cores.

2. Total cores interpretation

The softwear ESRI ArcMap™ version 10.0 has been used to interpolate the total cores dataset and to generate the maps enabling a spatial interpretation of the different parameters as the isotopic composition or the snow depth. Spatial interpolation estimates a function F(x) in which x=(x;y), at a point x_s of the surface thanks to known values of F in some m points of the sur surface x_i :

$$F(x_s) = \sum_{i=1}^{m} W_i \cdot X_i$$

Equation : Interpolation function. x_i : point of the surface with known value ; $F(x_s)$: interpolated value of the point x_p (x_p,y_p), m : number of points used for the interpolation, W_i: weigh of x_i point.

Several statistical methods exist to determine the weigh W_i of each of the m X_i points, the two most used in geology or soil sciences are the inverse distance weighted interpolation and the kriging. They consist in generating a surface grid from point data. The inverse distance weighted determines cell values using a linear weighted combination set of sample points. The weight assigned is a function of the distance of an input point from the output cell location : the greater the distance, the lower the weight. The inverse distance weighted function cannot be used for our dataset because the set of points is not dense enough. Kriging is a more useful interpolation method that assumes that the direction or distance reflects a spatial correlation that can be used to explain variations in the surface. The predicted values are derived from the measure of relationship in samples using sohisticated weighted average technique that will not be presented here. Unlike the inverse distance weighted function, the surface does not pass through the samples and the generated cell values can exceed the value range of samples. Several way exist to krige a dataset, the parameters we used in the kriging function in ArcMap are the following : Kriging method : ordinary, Semi-variogramm model : spherical, points build from the 12 first neighbourhood with a variable radius.

2.I. Snow depth

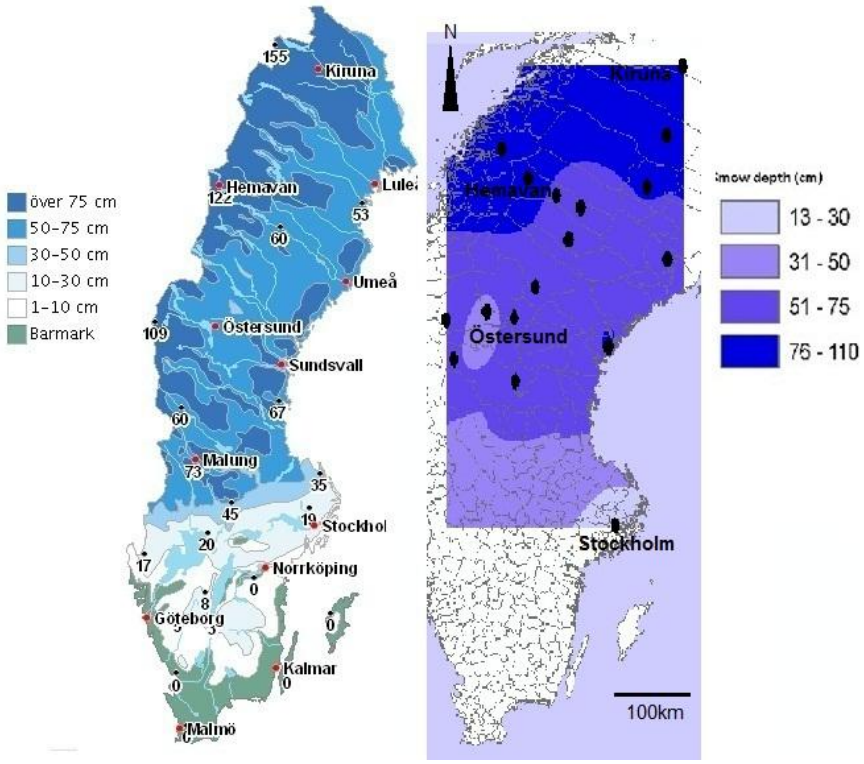

Figure 25 : Depth of the Swedish snowpack interpolated by the SMHI thanks to all their stations (a), and interpolated by kriging the dataset stemming from the collected total cores at the beginning march 2011 (http://www.smhi.se/klimatdata/meteorologi/sno)

The snow depth measured during the field campaign is plotted above and can be compared to the SMHI map of snow depth recorded on 15/03/2011. There is a good agreement between the two maps. Note, however, the depth measured in Abisko and Trondheim are not considered since their their low values are not representative of the local mean depth and was too much weighed in the interpolation method (figure 25).

2.II. Spatial variation of the isotopic composition

The spatial variation of the isotopic composition is calculated from the analysis of the total cores. The total cores collected in Östersund have leaked during the transfer and therefore we use the isotopic signature determined from the weighted mean of the high resolution cores.

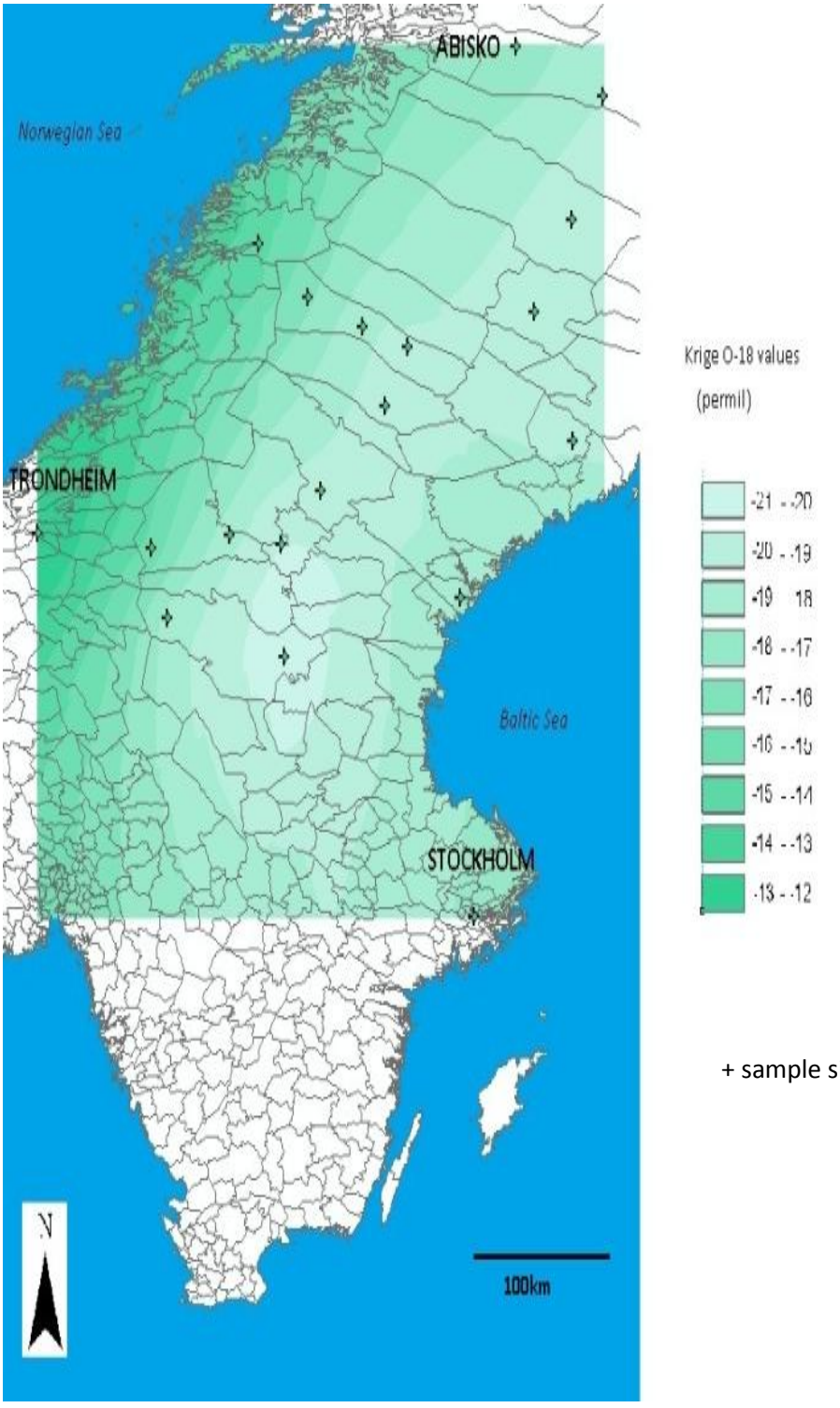

Figure 26 : Map of $\delta^{18}O$ interpolated thanks to kriging method in ArcGis over the field study area. The $\delta^{18}O$ data are derived from the total cores collected during the field trip in early march 2011. The darker green are more enriched in ^{18}O whereas the lighter green are more depleted in ^{18}O

Similar to the interpolation of the snowpack depth, the isotopic composition of the total cores has been interpolated over the area using the kriging method in ArcGIS. This map represents the integrated $\delta^{18}O$ over the whole thickness of the snowpack.

Only the $\delta^{18}O$ is shown here because the δD map is similar. Indeed, deuterium and ^{18}O have the same physical behavior during precipitation.

The highest $\delta^{18}O$ value is on the most western part of the studied area, in Trondheim (-9,31‰) and the lowest one is situated in Ljusnedal (-22,07‰) in the center of the studied area.

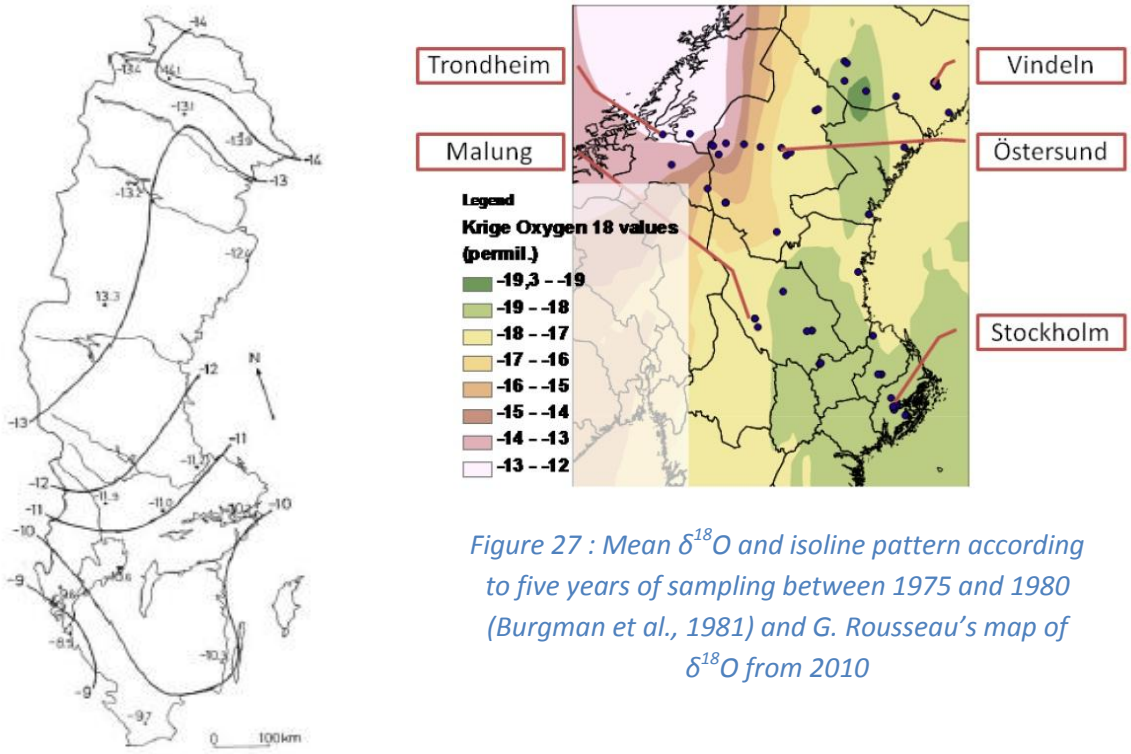

Figure 27 : Mean $\delta^{18}O$ and isoline pattern according to five years of sampling between 1975 and 1980 (Burgman et al., 1981) and G. Rousseau's map of $\delta^{18}O$ from 2010

According to Burgman samplings between 1975 and 1980 which represents the winter months December-January-February snow falls, the isotopic gradient is mainly latitudinal (figure 27). The gradient we can observed on the map representing the March 2011 $\delta^{18}O$ values is likely longitudinal, perpendicular to the western Norwegian coast. Indeed, the higher the distance is from the western coast ; the more depleted in ^{18}O are the precipitations. This shows the Atlantic origin of the air masses enriched in oxygen-18 that is depleted in ^{18}O when it precipitates on its path along the longitude. The map derived from 2011 dataset confirmed the same phenomenon reported by G. Rousseau from 2010 study (figure 27).

We can also observe that the total cores collected on the eastern part are higher than expected considering the westerly air masses effect. We can assume that there is a mixing of the Atlantic air masses with the Baltic air masses that arises the $\delta^{18}O$ on the east coast.

2.III. Transects

Two transects along the latitude, sub-perpendicular to the western Scandinavian have been done during the field trip in early March 2011. One of those is the same G. Rousseau did last year, between Trondheim and Härnösand (near Sundsvall) roughly around 63,5±1° N in order to compare the same transect during two consecutive years negative NAOi. The other transect has been done up north between Mo I Rana in Norway and Kryklan (near Umeå), a transect oriented NW-SE, perpendicular to the west coast.

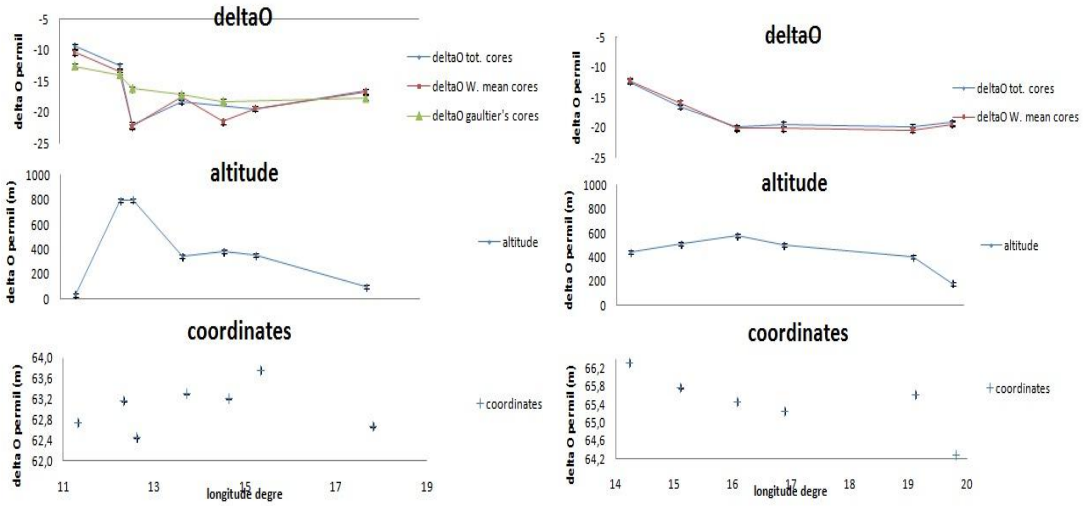

Figure 28 : West-East transect, between Trondheim and Härnösand (Sundsvall). Top : $\delta^{18}O$ (blue line represents the total cores data, the red line represent the weighted mean data and the yellow line represent G. Rousseau's data, middle : altitude (m) and bottom : location (a). NWW-SEE transect between Mo I Rana (Norway) and Kryklan (near Umeå, Sweden). Top : total cores $\delta^{18}O$, middle : altitude (m) and bottom : location (b).

The data collected during the winter 2011 along the transect E-W are plotted with the data collected in winter 2010. We can observe the same trend between the two years. We can observe several zones, a first one where the $\delta^{18}O$ is strongly decreasing roughly between 11°E (Trondheim) where $\delta^{18}O_{2011}$ = -9,3‰ and 12,6°E (Ljusnedal) where $\delta^{18}O_{2011}$ reaches -22,5‰, a second one where the $\delta^{18}O$ increases with longitude, between 12,6°E and 13,7°E (Mörsil) where $\delta^{18}O_{2011}$ = -18,3‰. There is a depletion at longitude 14,6°E (Östersund) and then the $\delta^{18}O_{2011}$ increases slightly up to longitude 17,8°E (Kryklan) close to the Baltic Sea.

The second transect between Mo I Rana and Kryklan has relatively the same trend as the other transect between Trondheim and Härnösand but is a bit smoother. We can

observe a zone where the $\delta^{18}O$ is more strongly decreasing with the distance from Mo I Rana (14,2°E) to Nordanås (16,1°E). The evolution between Nordanås and Arvidsjaur (19,1°E) is almost flat and then increases up to Kryklan (19,8°E).

a. Altitudinal effect

The water vapor coming from the Atlantic Ocean is enriched in oxygen-18, that is likely why the $\delta 18O_{2011}$ measured in Trondheim (11°E) is so high. The higher altitude between Trondheim and Mörsil induces a higher precipitation rate causing the strong decrease of the $\delta^{18}O_{2011}$ between 11°E and 12,6°E. This strong decrease of $\delta^{18}O_{2011}$ is also due to the altitudinal effect. This altitudinal effect is temperature and pressure-related. According to the J.R. Gat et al. study in 2000, this altitudinal influence leads to an isotopic gradient ranging from -0,2‰/100m -0,6‰ for $\delta^{18}O$. The isotopic gradient has been calculated on both wind and lee side of these Swedish mountains. The gradient reaches -0,4‰/100m on the wind side and -0,8‰/100m on the lee side. Therefore, the altitudinal effect is not absolute and depends on the climate dynamics.

b. Precipitation rate over the transect

Besides the same trend in 2010 and 2011 plots, we can observe that the signal in 2011 is stronger than in 2010. According to the data recorded by the Swedish Service Meteorological and hydrological Institute (www.smhi.se), the snow pack was thicker in winter 2011 than in winter 2010 in over the transect (figure). For example, is Storlien, 20km away from Stor-Ulvan (representative of this area), the snow depth was 147cm in March 2011 whereas it was 97cm in March 2010 (given than the snow pack started to melt after March for both years).

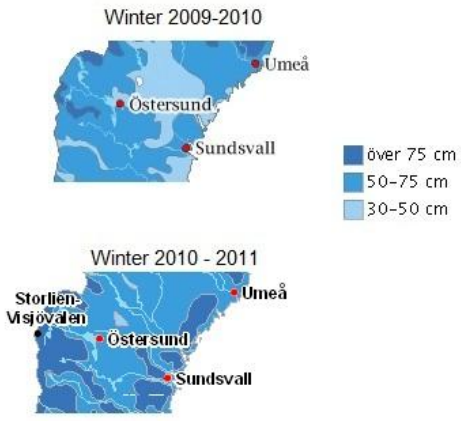

Figure 29 : comparison of the snow depth map in March 2011 and March 2010 over the area covering the transect. (Service Meteorological and Hydrological Institute, www.SMHI.com)

The precipitation rate was therefore higher in winter 2011 than in winter 2010. This potentially explains the gradient in winter 2011 being stronger than the winter 2010.

c. Westerly air masses effect

The $\delta^{18}O$ is globally decreasing from the west to the east showing that the distillation of Rayleigh partly governs the west-east evolution the isotopic composition (figure 1). The first rain released by the cloud enriched in oxygen-18 has a high $\delta^{18}O$ ($\delta^{18}O_{tronheim}$ = -9,3‰). The remaining vapor after the first precipitation is therefore depleted in heavy water isotopes and the following precipitations will therefore be depleted in oxygen-18 :

$$R = R_0 f^{\alpha-1}$$

R_0 : initial vapor isotope ration ; R : isotope ratio f residual vapor in the cloud ; f : residual vapor reservoir ; α : fractionation factor

Equation : Rayleigh distillation equation

The mean longitudinal gradient has been calculated for winter 2011 and winter 2010 by determining a regression line. The two gradients are almost similar, indeed, in 2011, $\Delta\delta^{18}O/\Delta$°long. = -0,75‰/°long. and is it equal to -0,74‰/°long in 2010. At about 63,5°N, considering that the transect is perfectly parallel to the parallels, these gradients are equal to -1,5‰/100km. The gradient for the transect between Mo I Rana and Kryklan has also been calculated. It has not been calculated as a function of longitude because it is not parallel to latitudes but it has been directly calculated as a function of the distance between Mo I Rana and Kryklan. In that case, the transect is equal to -1,54‰/100km, which is very close to the two other gradients.

3. Cut cores interpretation

The $\delta^{18}O$ profiles of the high resolution cut cores were plotted as well as the $\delta^{18}O$ profiles of the corresponding low resolution cut cores in order to verify if the two signals were similar and then validate the evolution of the high resolution core (figure 30).

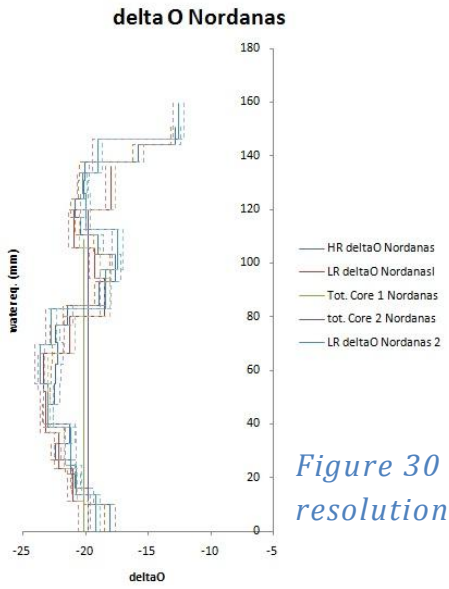

Figure 30 : $\delta^{18}O$ of high resolution and low resolution cut cores in Nordanås

For example, the Nordanås high resolution and low resolution fit perfectly to each other. Though, one of the low resolution cores did not record the signal at the top of the core. But the trend is almost the same and proves that there is a continuity of the isotopic signal at a local scale. This enables the possibility to validate the evolution of $\delta^{18}O$ in the snow pack for this site.

Concerning another example in Laxbacken (annexe 2), the correspondence between the high resolution and the low resolution is not as obvious as with Nordanås samplings. Actually, the low resolution core misses the bottom signal we can observe on the high resolution profile and the profile is smoothed by lower resolution. Then we can validate the entire high resolution core in Laxbacken.

The high resolution of all the sampling sites have been validated by this method. All sites show good agreement but Mörsil profile whose low resolution and high resolution was too different to be validated. Still, this gives good support that the low resolution samples maintain much of the data collected regarding the total snow pack as the high resolution samples.

3.I. Large scale trend within cut cores profile

All the validated profiles over the studied area were put together in order to highlight any large scale pattern in the temporal variability of the isotopic composition in the different sampling sites. Note that Mörsil is not plotted because its profile was not validated and Trondheim is not plotted either because the snow depth was too low (13cm) (annex 3).

Due to logistic constraints, the data from the stations have not been obtained and therefore, it was not possible to attempt to date the peaks with precision in this current study.

Nevertheless, we can observe, regarding the cores, that there is the same pattern for most of the profiles (Kiruna, Arvidsjaur, Mo I Rana, Nordanås, Laxbacken, and Blaiken). Firstly there is a depletion phase of the precipitation which reaches a first minimum. Then the $\delta^{18}O$ increases again before there is a second depletion phase. Finally the $\delta^{18}O$ increases again. Some of the profiles miss a part of the evolution (Abisko, Hallaxåsen, Stor-Ulvan, Östersund and Sveg), and some others record more like in Hemavan. The profiles corresponding to the eastern part of the studied area show a different pattern compared to the others collected across Sweden (Stockholm, Kryklan, Härnösand).

According to the data from SMHI, the snowpack began to be continuous from the 10/11/10, therefore we assume that each core is a record from the beginning of November 2010 to March 2011.

3.II. $\delta^{18}O$ profiles, an illustration of winter temperature

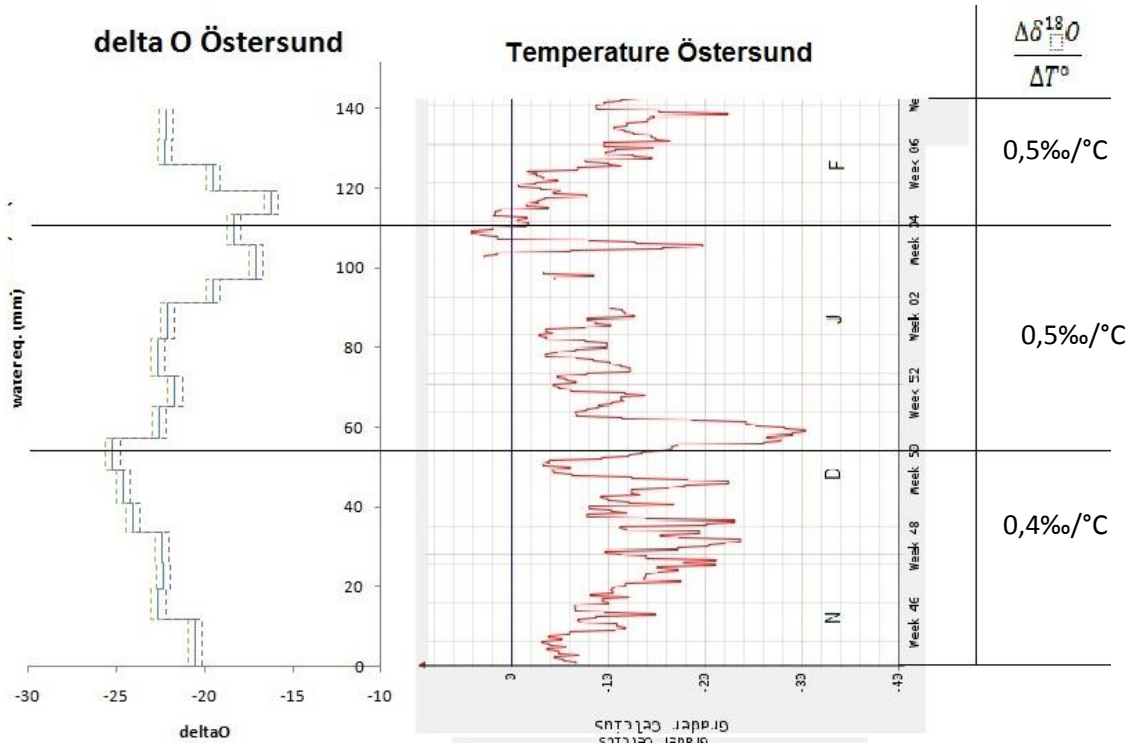

Figure 31 : comparison $\delta^{18}O$ profile and Temperature in Östersund and the gradient corresponding to temperature effect.

As said in the previously, the peaks of the profiles could not be dated. However, it is obvious that there is a correlation between the temperature profiles over Sweden from November until March and the isotopic profiles (figure 31). In addition, according to J.G Gat (2000), the temperature effect equation in isotopic composition of precipitations should be as follows (derived from ClaudiuS-Clapeyron equation and the equation illustrating the temperature dependence of the fractionation) :

$$\frac{\Delta\delta^{18}O}{\Delta T°} = 0{,}4‰/°C$$

Equation : theoretical equation of the temperature effect. (J.R. Gat et al., 2000)

The gradients have been calculated by correlating the peaks on both profiles. The values of the temperature peak have been obtained by averaging the temperature of 15 days surrounding the peak because of the daily variability of temperature.

The temperature effect for Östersund core ranges from 0,4‰/°C to 0,5‰/°C which relatively close to 0,4‰. The gradients have been calculated for other sites over Sweden and it appeared the gradient ranges from 0,2‰/°C to 0,7‰/°C because of the uncertainties due to the approximate dating of the peaks.

The investigation of the isotopic composition of the snowpack in Sweden reflects the temperature evolution in this area. Furthermore, it shows that the theoretical temperature effect is observable in the snowpack in winter 2011 (figure 31).

3.III. Temperature versus Nao during Winter 2011

As it is presented in the chapter C.3.III., there was a negative anomaly in the temperature in February 2011. Regarding the North Atlantic Oscillation, this cold event corresponds to a fast inversion from negative to positive (-0,88 in January, 0,7 in February). According to the literature, the positive NAO phase corresponds to wetter and warmer temperature in North of Europe. This cold event corresponding to a positive NAO in February 2011 shows that the climatic patterns such as air masses trajectories or temperature does not react instantaneously to an abrupt transition from a negative phase to a positive phase. Though, this cold event can be linked to this abrupt transition which might have generated a disturbance.

G. Conclusion

The field campaign which occurred in March 2011 to collect snow samples over the northern half of Scandinavia provided a huge dataset of the isotopic composition of the snowpack of winter 2011. As Rousseau G. in winter 2010, the stable water isotopes in the snowpack revealed themselves as interesting information resources to investigate climate issues.

The analysis of the isotope composition was performed by the laser spectrometer from Los Gatos Research and enabled the measurement of more than 700 samples in about two weeks. This new technology has a big potential but experimental protocol and post-processing procedure have still to be improved to insure that the measurement obtained by the LGR-LS achieve a similar accuracy and precision as mass spectrometry.

Winter 2011 was characterized, as well as winter 2010 by a negative NAOi, low temperatures and a high precipitation rate. This current study highlighted an East-West isotopic gradient illustrating the atlantic origin of the water vapor generating the precipitations over Sweden in winter 2011. This gradient is observable in winter 2011 and winter 2010 on the transect between Trondheim and Sundsvall and is observable more generally on the entire studied area. The mean gradient over the transects for both winters seems to be constant and equal to -1,5‰/100km.

This gradient corresponding to a continental effect shows that negative phase of NAO are not systematically corresponding to cold and dry air masses coming from Siberia and proves therefore the limit of the teleconnection to explain climate dynamic over the North of Europe.

In addition, the temporal variability of the stable water isotopes content in the snowpack has a good agreement with the temperature over Sweden between November 2010 and March 2011. The calculated temperature gradient in snow samples in winter 2011 proved that the temperature effect is an important influencing parameter on the isotopic composition in precipitations this winter.

Outlook

This current study showed that NAO was not the most important parameter to govern the temperature and therefore the isotopic composition in winter 2011. An interesting investigation could the study of the temperature over several years subtracted from its seasonality effect in order to precise the importance on NAO in the temperature in North of Europe.

Furthermore, the data recorded in the weather stations near the sample sites could not been obtained. This therefore limited the interpretation of the results. An investigation of this dataset supported by a larger meteorological data bank.

Test batches have been analyzed in order to investigate the memory effect that still affects the accuracy in measurements by the laser spectrometer. We did not have time to focus on this aspect and the dataset derived from the measurements of these test batches should be used in developed statistical investigation in order to minimize this error factor.

Bibliography

Barnston A. G., and R. E. Livezey, (1987), *Classification, seasonality and persistence of low-frequency atmospheric circulation patterns*. *Mon. Wea. Rev*, 115, 1083-1126.

Burgman, J.O., et al. (1981*), "Oxygen 18 - Variation in monthly precipitation over Sweden.*" Uppsala

Cattiaux et al. (2010), Winter 2010 in Europe : a cold extreme in a warming climate, Geophysical Research Letters, Vol. 37, Paris

Dansgaard, Willi.(1964), "Stable isotopes in precipitation." *Tellus* : XVI: 436–468.

Gat J.R. et al (2000), *Stable water isotope processes in the water cycle*, vol. 2, chapt. 3, Environmental isotopes in the hydrological cycle : principles and applications. Groningen

IAEA.(2009), *Laser Spectroscopy Analysis of LiquidWater Samples for Stable Hydrogen and Oxygen Isotopes. Performance Testing and Procedures for Installing and Operating the LGR DT-100 Liquid Water Isotope Analyzer*. Vienna,: ISSN 1018-5518,, 2009.

Rodhe A. (1987). *The Origin of the Streamwater.* Uppsala,

Rousseau G. (2010), *Caractérisation de l'hiver 2009/2010 par les isotopes stables de l'eau dans le manteau neigeux en Scandinavie.* Master thesis, Stockholm

Slabunov. A., (1999) "Late Archaean Subduction and Collision Events in the Crustal Evolution of the Eastern Fennoscandian/Baltic Shield." Journal of Conference Abstracts, Vol. 4, No. 1, Symposium A08, Early Evolution of the Continental Crust

Sturm C et al. (2010), *First results with the laser-spectrometry Liquid Water Isotope Analyser: considerations on experimental protocol and analytical post-processing*, Stockholm.

Thompson, D., and J. Wallace (1998), *The Arctic Oscillation signature in the wintertime geopotential height and temperature fields*, Geophys. Res. Lett., 25(9), 1297–1300.

Annex

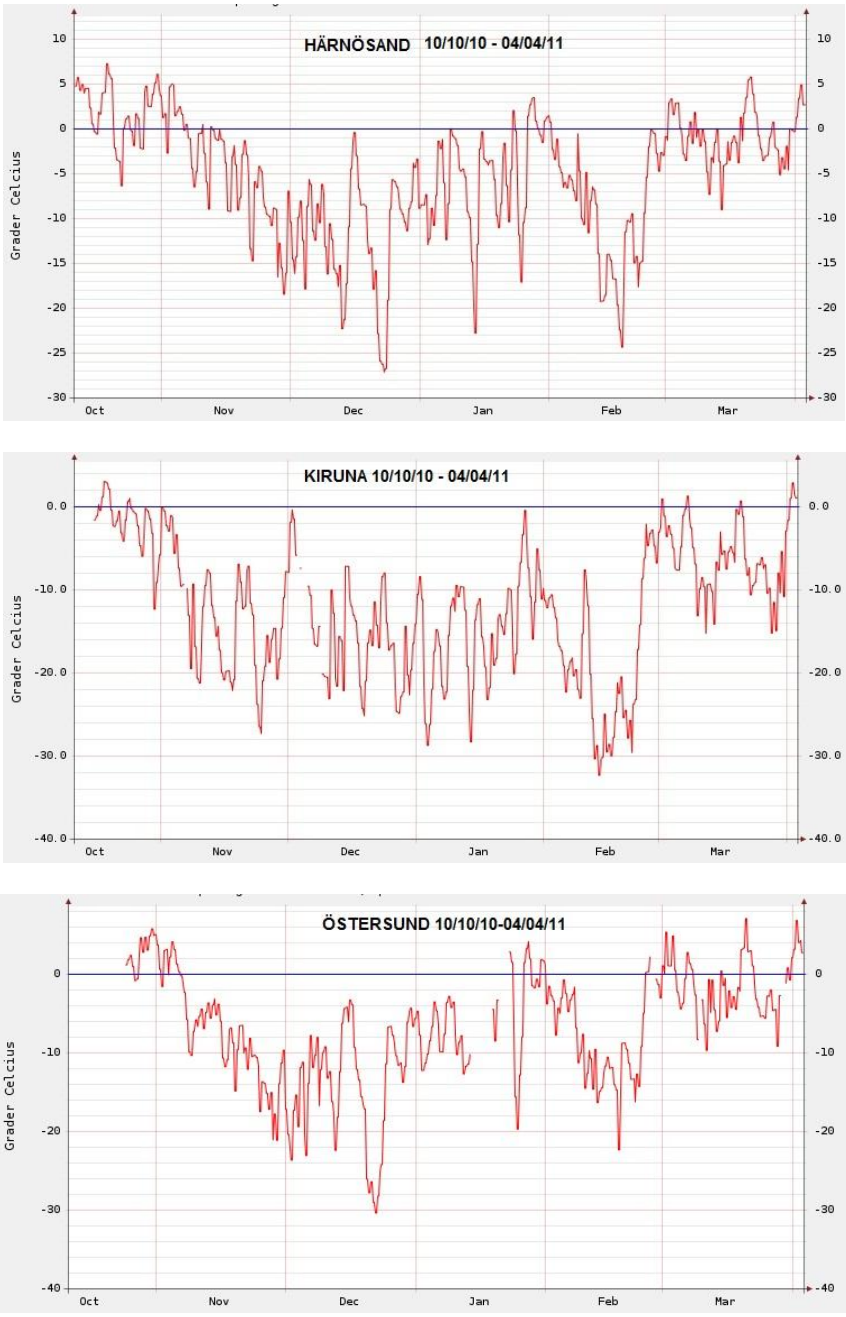

Annex : temperature in Östersund (63,2°N 14,6°E, center of the studied area), in Kiruna (67,8°N 20,3°E, north of the studied area) and Härnösand (62,7°N 17,8°E, south-east of the studied area) from the 10th of November 2010 to the 4th of April 2011. (Service Meteorological and Hydrological Institute, www.SMHI.com

Annex

SITE 1														
date	12 March 11	n		res (m)	length (cm)	N	E	density	deltaD ‰	deltaO ‰	comments			
nb cores high res		1	KRY1	0,025	57,5	64,282	19,812	0,231	-133,326	-18,992	sampled on a bulk, irregular ground, vegetals			
nb cores low res		1	KRY2	0,05	75	64,282	19,812	0,234	-132,879	-18,771	sampled on a bulk, irregular ground, vegetals			
nb of T cores		2	KRY3		66	64,282	19,812	0,176	-130,977	-18,691	sampled on a bulk, irregular ground, vegetals			
			KRY6		57	64,282	19,812	0,215	-133,253	-18,481	sampled on a bulk, irregular ground, vegetals			
sample	depth	sample weig	density (g.cr	deltaD ‰	deltaO ‰	wat eq. (mm	wat eq cum.	comments						
KRY1-S1	57.5-55	15	0,153	-154,983	-20,684	3,820	132,672	fine snow						
KRY1-S2	55-52.5	17	0,173	-150,587	-20,512	4,329	128,852	fine snow						
KRY1-S3	52.5-49	34	0,247	-122,998	-16,459	8,658	124,523	ice layer						
KRY1-S4	49-46	22	0,187	-149,380	-21,177	5,602	115,865	normal snow						
KRY1-S5	46-43.5	26	0,265	-148,170	-20,773	6,621	110,263	normal snow						
KRY1-S6	43.5-40.5	26	0,221	-133,770	-17,711	6,621	103,642	ice pieces						
KRY1-S7	40.5-38	28	0,285	-122,264	-17,169	7,130	97,021	medium cristals and ice layer						
KRY1-S8	38-35.5	25	0,255	-123,514	-17,293	6,366	89,891	medium cristals						
KRY1-S9	35.5-33	29	0,295	-129,200	-17,935	7,385	83,525	medium cristals						
KRY1-S10	33-30.5	22	0,224	-133,059	-18,154	5,602	76,140	medium cristals						
KRY1-S11	30.5-28	29	0,295	-133,046	-18,521	7,385	70,537	medium cristals						
KRY1-S12	28-25.5	29	0,295	-136,854	-19,186	7,385	63,153	medium cristals						
KRY1-S13	25.5-23	31	0,316	-143,875	-20,162	7,894	55,768	medium cristals						
KRY1-S14	23-20.5	15	0,153	-150,525	-21,296	3,820	47,874	medium cristals & mass loss						
KRY1-S15	20.5-18	29	0,295	-151,249	-21,684	7,385	44,054	medium cristals						
KRY1-S16	18-15.5	22	0,224	-141,127	-21,317	5,602	36,669	big cristals						
KRY1-S17	15.5-13	30	0,306	-127,352	-19,137	7,639	31,067	big cristals						
KRY1-S18	13-10.5	19	0,194	-120,774	-19,092	4,838	23,428	big cristals						
KRY1-S19	10.5-8	24	0,244	-116,288	-18,627	6,112	18,589	big cristals						
KRY1-S20	8-5.5	16	0,163	-118,075	-18,185	4,074	12,478	big cristals	dens integ	deltaD ineg	deltaO integ			
KRY1-S21	5.5-0	33	0,153	-114,008	-17,175	8,403	8,403	big cristals	0,2307331	-133,32554	-18,992424			

Annex 1 : Table of all the data collected to obtain $\delta^{18}O$ and δD profile in snowpack.

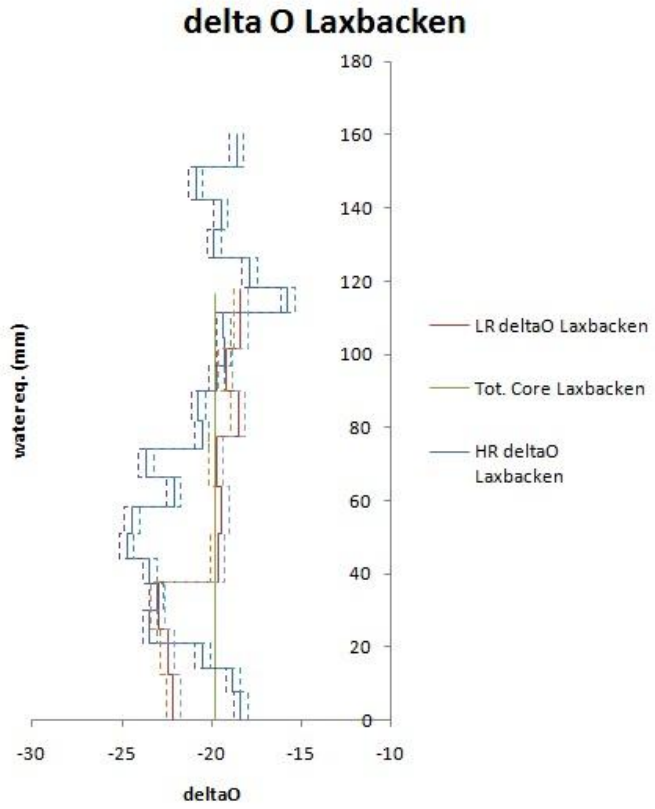

Annex 2 : $\delta^{18}O$ of high resolution and low resolution cut cores in Laxbacken

Annex

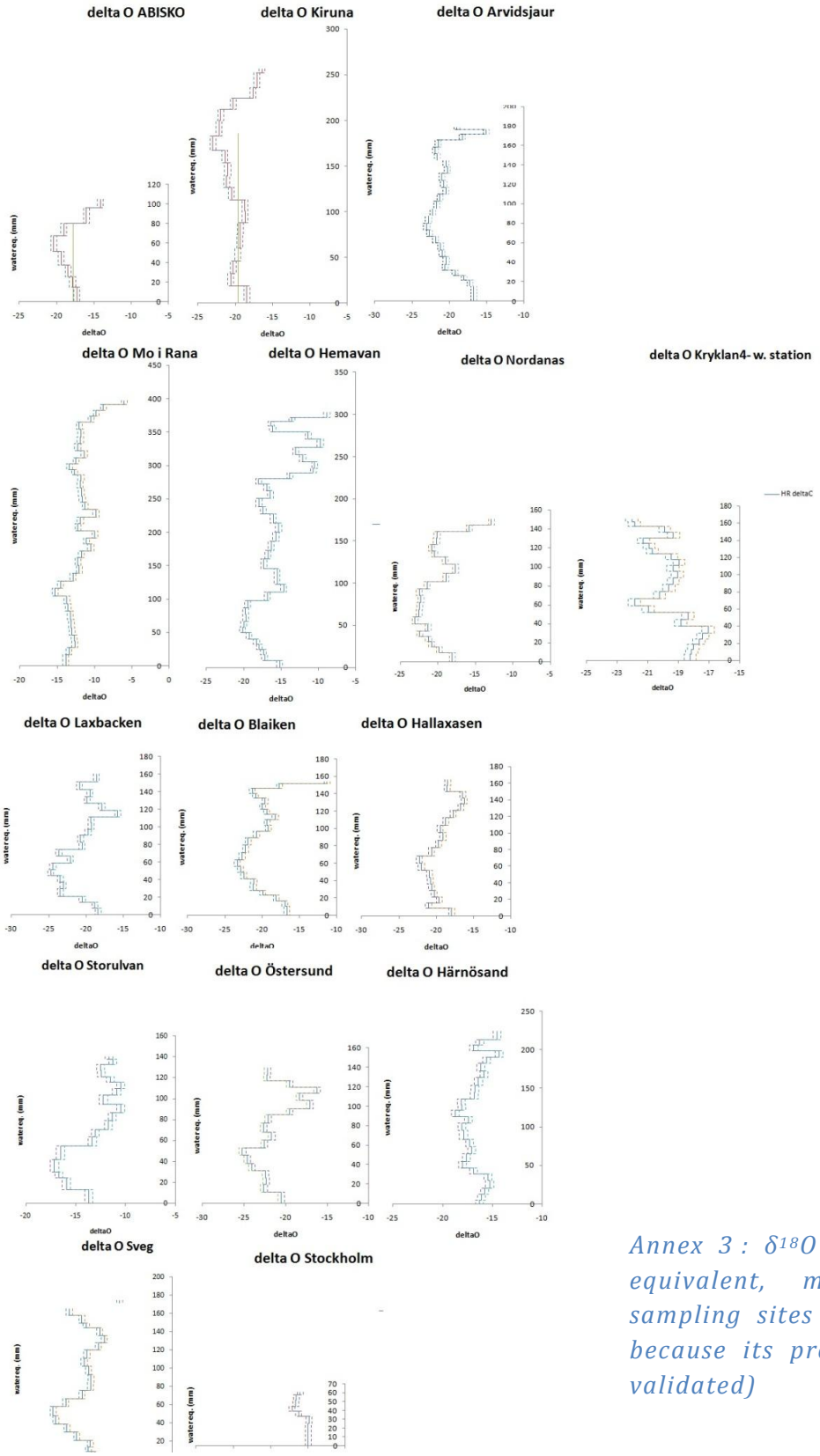

Annex 3 : $\delta^{18}O$ profiles (in water equivalent, mm) of all the sampling sites (Mörsil is missing because its profile has not been validated)

Résumé

La composition isotopique des précipitations dépend de paramètres tels que l'origine des nuages dont elles sont issues. La trajectoire des vents amenant les masses d'air sur le nord de l'Europe est en partie influencée par l'oscillation Nord Atlantique dont l'indice associé était très négatif ces deus derniers hivers, 2009-2010 et 2010-2011. En outre, ces deux hivers sont caractérisés par des températures basses persistantes et des précipitations importantes.

Des échantillons du manteau neigeux datant de l'hiver 2010-2011 ont été prélevés en Suède et en Norvège entre les latitudes 62°N et 68°N avant les premières températures positives, entre le 4 et le 12 mars 2011. Des carottes de neiges ont été échantillonnées sur 20 sites répartis sur une zone d'une superficie de 350.000km² représentant un peu plus de 700 échantillons. Ils ont été amenés au département de géologie et de géochimie de l'université de Stockholm afin de mesurer leur composition isotopique, δD et $\delta^{18}O$. D'autres paramètres comme la profondeur de neige ou la taille des grains ont aussi été relevés durant cette campagne.

Les échantillons ont été analysés avec un spectromètre laser de Los Gatos Research (LGR-LS), machine commercialisée depuis moins de 4 ans. Cette nouvelle machine permet une analyse plus rapide et moins chère de la composition isotopique d'échantillons d'eau par rapport au spectromètre de masse. Cependant, son évaluation en janvier 2010 a révélé des problèmes de précision, d'effet mémoire et de dérive. Une attention particulière a donc été portée sur le protocole expérimental et sur le traitement post-analyse pour minimiser ces erreurs.

Les données issues de l'analyse des échantillons sont utilisées pour étudier les feedbacks entre la surface continentale et la dynamique atmosphérique. G. Rousseau a montré l'an dernier l'importance de l'effet des masses d'air provenant de l'ouest sur la composition isotopique du manteau neigeux en Scandinavie. Ce phénomène se retrouve dans la modélisation du programme $REMO_{ISO}$ développé par C. Sturm. Les données de cet hiver montrent un gradient encore plus important que celui de l'an passé due à cet effet continental.

En outre, ces données vont permettre de caractériser et de comprendre cet hiver 2010-2011, en étudiant la variabilité temporelle comme spatiale de la composition isotopique de la neige.